Science Advances
AAAS

advances.sciencemag.org/cgi/content/full/7/12/eabe9459/DC1

Supplementary Materials for

A towering genome: Experimentally validated adaptations to high blood pressure and extreme stature in the giraffe

Chang Liu, Jianbo Gao, Xinxin Cui, Zhipeng Li, Lei Chen, Yuan Yuan, Yaolei Zhang, Liangwei Mei, Lan Zhao, Dan Cai, Mingliang Hu, Botong Zhou, Zihe Li, Tao Qin, Huazhe Si, Guangyu Li, Zeshan Lin, Yicheng Xu, Chenglong Zhu, Yuan Yin, Chenzhou Zhang, Wenjie Xu, Qingjie Li, Kun Wang, M. Thomas P. Gilbert, Rasmus Heller*, Wen Wang*, Jinghui Huang*, Qiang Qiu*

*Corresponding author: Email: qiuqiang@lzu.edu.cn (Q.Q.); huangjh@fmmu.edu.cn (J.H.); wwang@mail.kiz.ac.cn (W.W.); rheller@bio.ku.dk (R.H.)

Published 17 March 2021, *Sci. Adv.* **7**, eabe9459 (2021)
DOI: 10.1126/sciadv.abe9459

This PDF file includes:

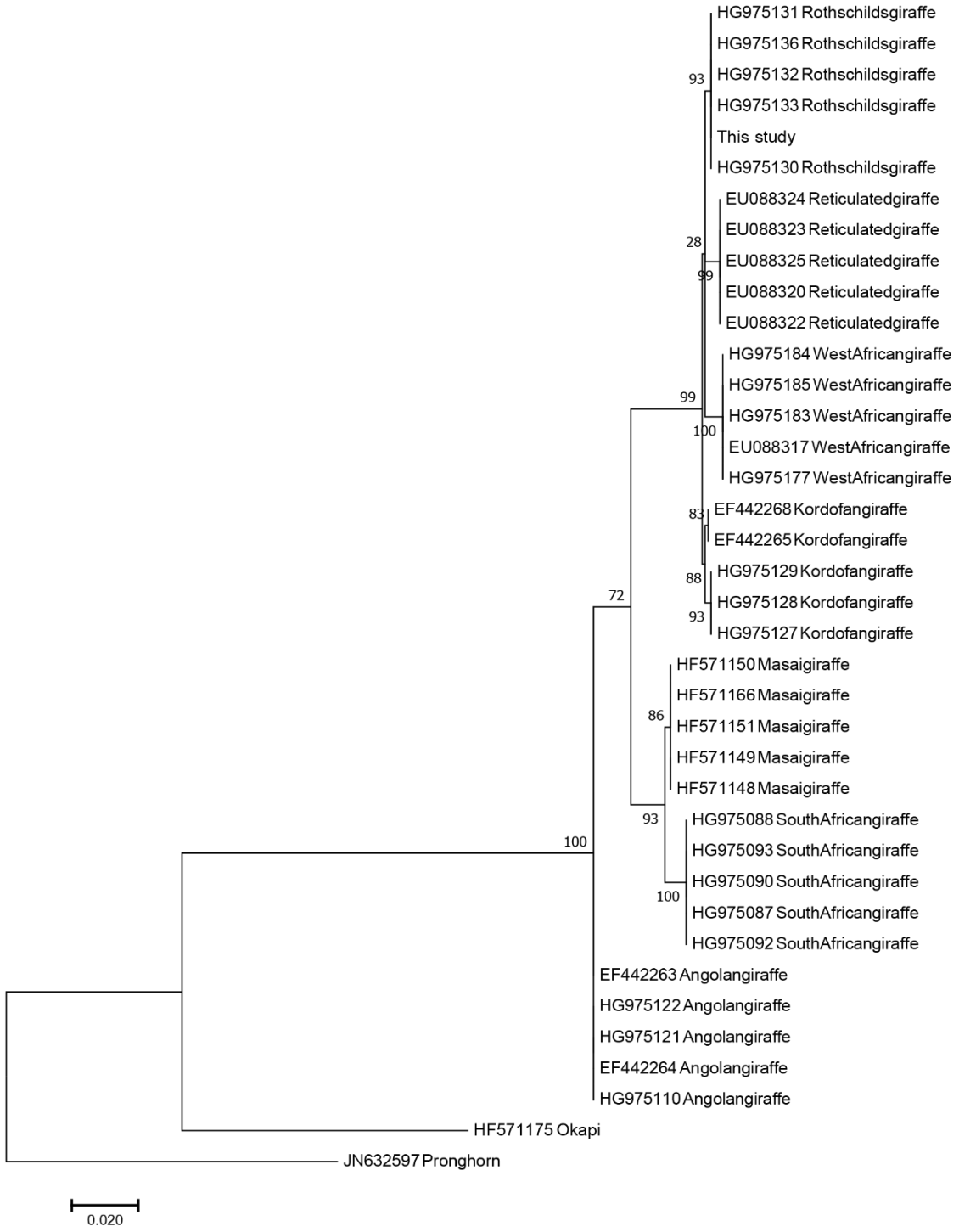

Fig. S1| Taxonomic identification based on cytochrome b (*Cytb*) gene. *Cytb* sequences of 160 giraffe individuals and two out group species from the previous study (*56*) were used for analysis, and we showed only five giraffe individuals for each population here. The phylogenetic tree suggests our sample (This study) is highly similar to other Rothschild's giraffes with high support (UFB value=93).

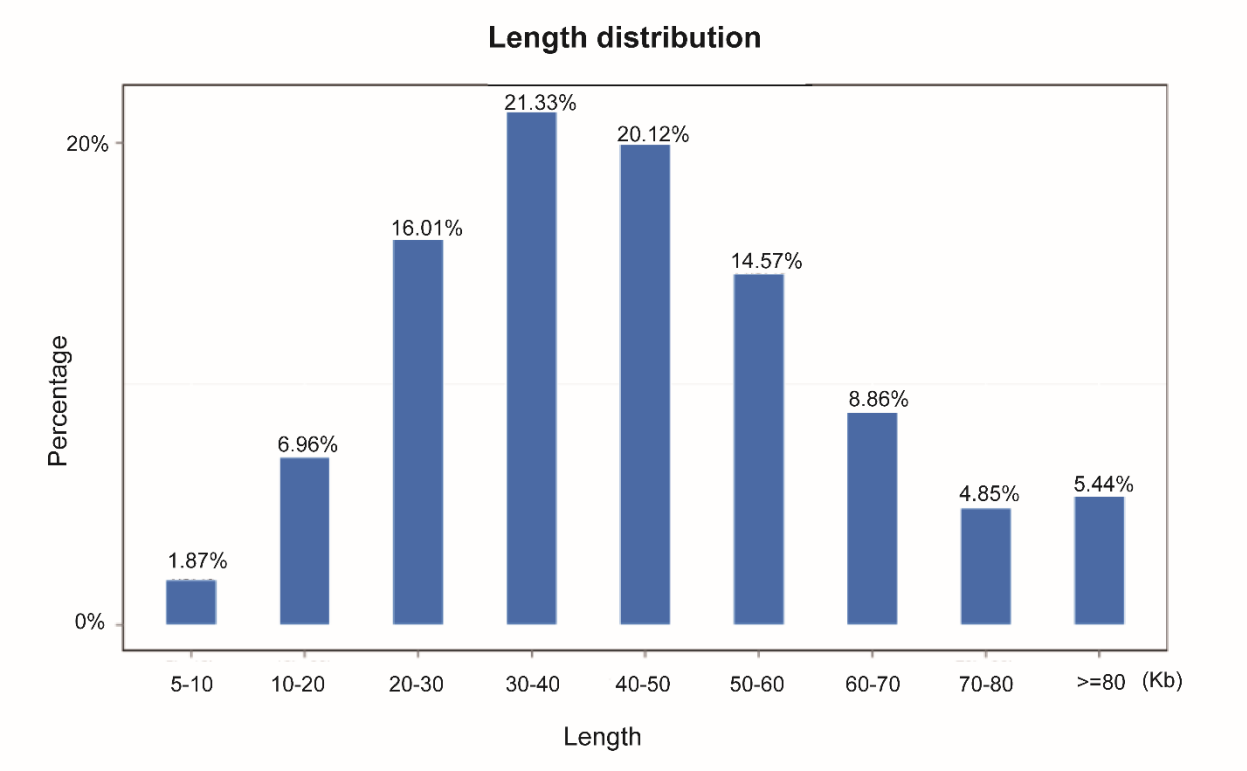

Fig. S2 | The length distribution of filtered Oxford Nanopore long-reads. We obtained 140.56 Gb clean data (4,124,698 clean reads), with an average length of 34,078 bp, max length of 1,043,973 bp and N50 length of 41,773 bp.

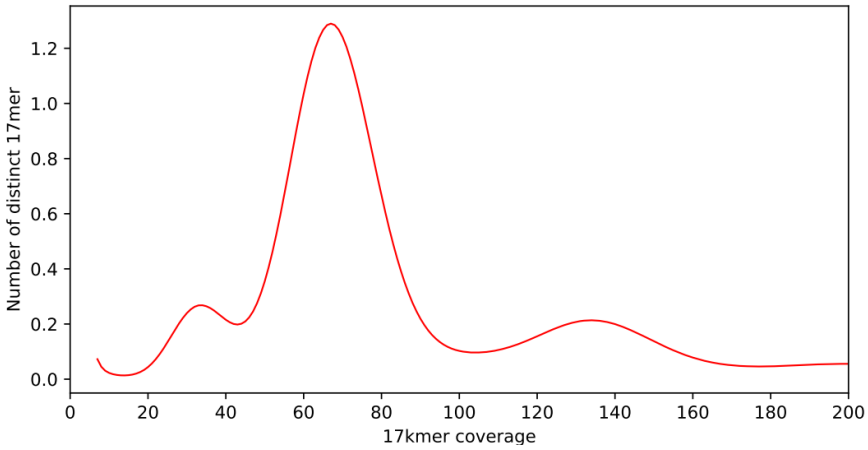

Fig. S3 | *K*-mer (k=17) distribution of the giraffe genome. The estimated genome size, based on 17-mer analysis, is 2.54 Gb, with estimated heterozygosity of 0.003.

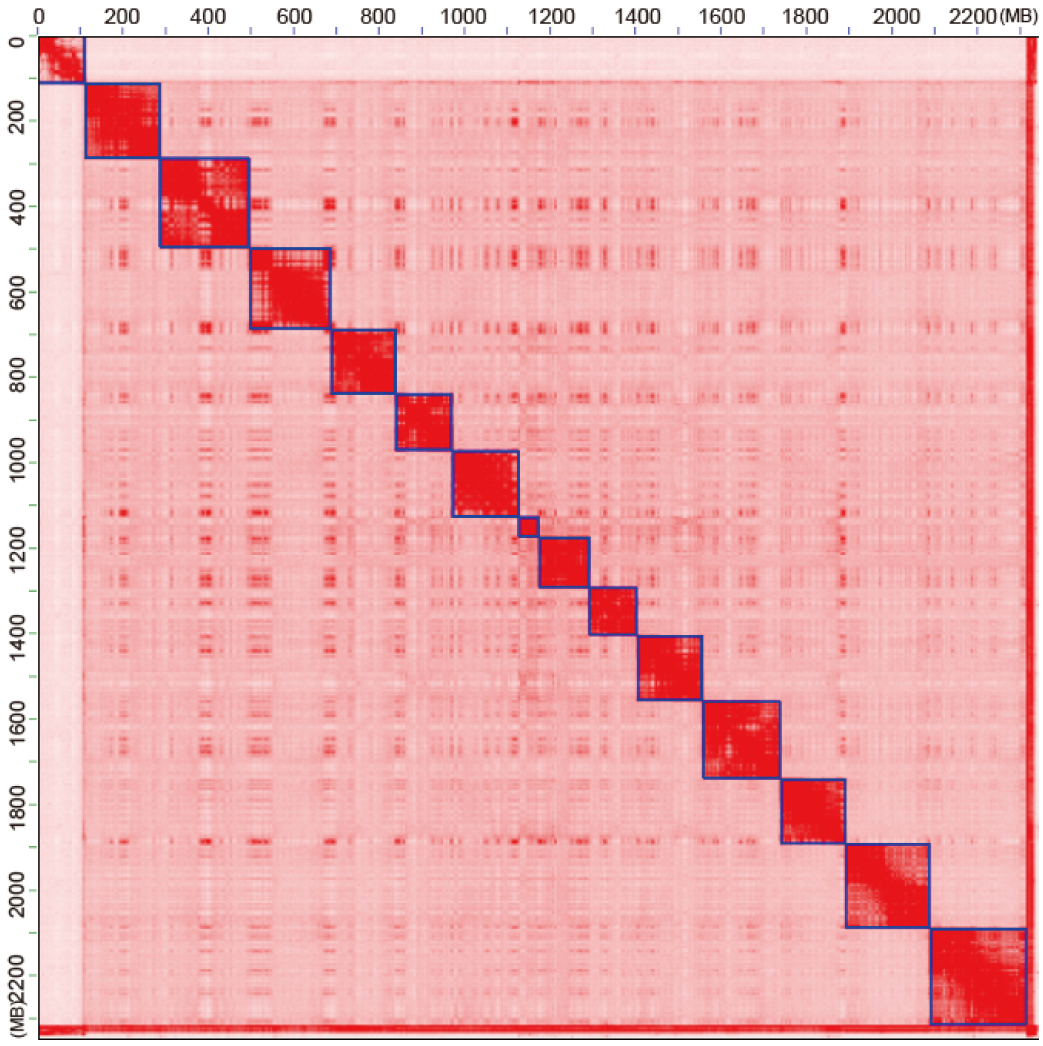

Fig. S4| Hi-C linkage density heat map of the giraffe chromosome assembly. It shows that edges of chromosomes are very clear.

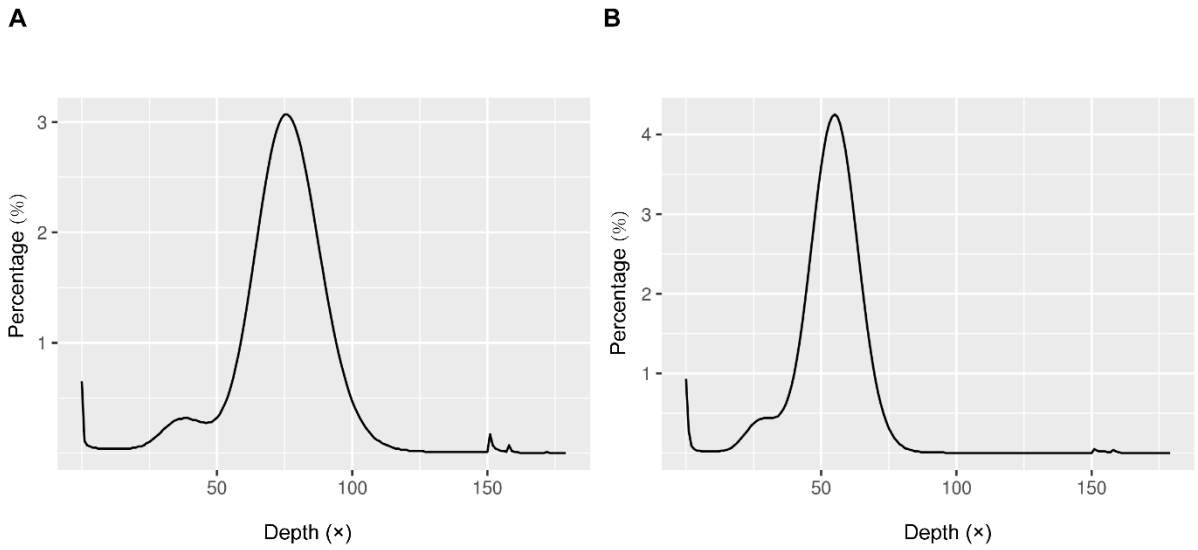

Fig. S5| Distributions of read depth across the giraffe genome. Both the Illumina Hiseq and Nanopore reads used for genome assembly were mapped back to the genome. Average mapping depths of the Illumina **(A)** and Nanopore reads **(B)** are 79 × and 54 ×, respectively.

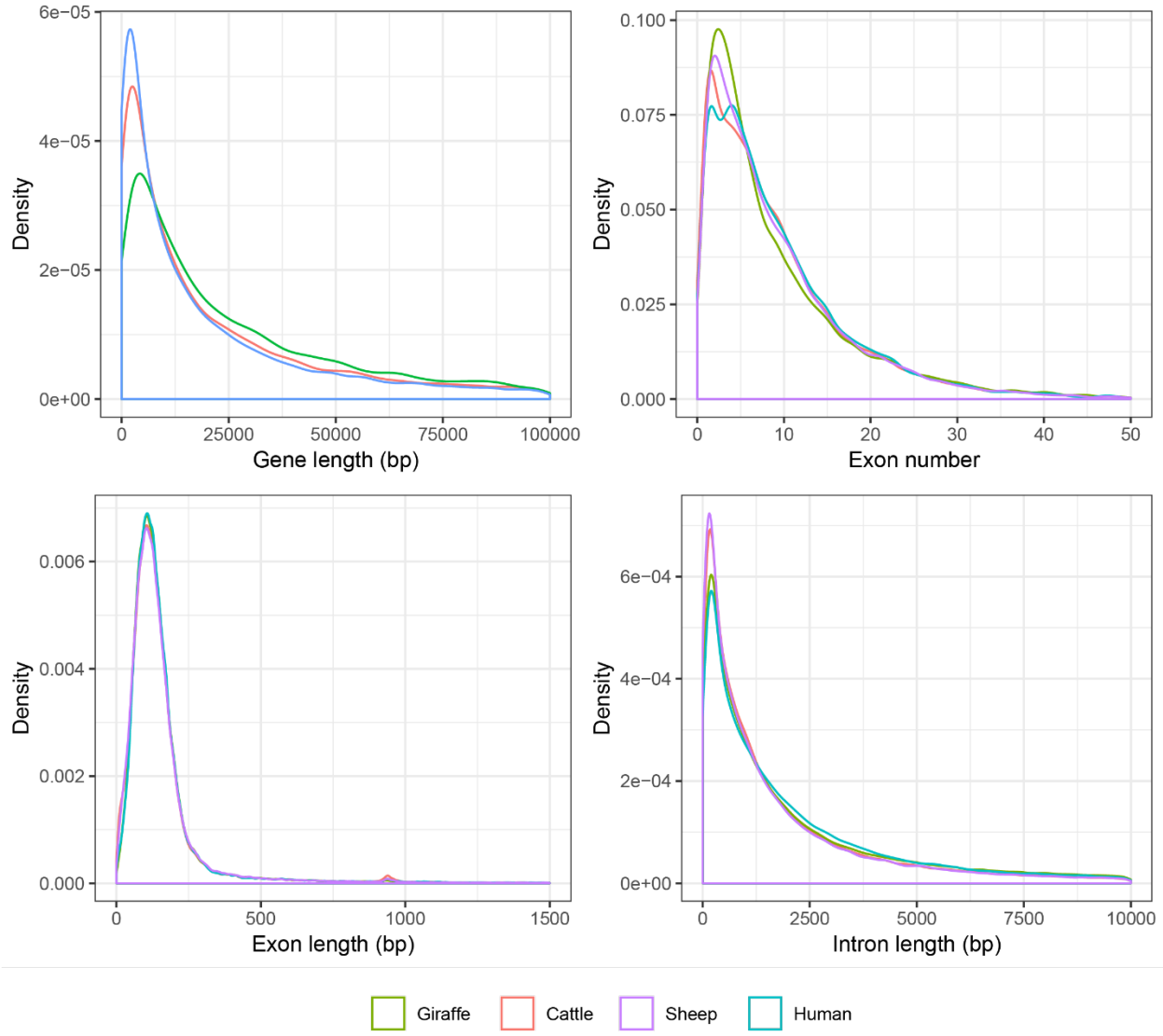

Fig. S6| Evaluation of gene annotations. Gene length **(A)**, exon number **(B)**, exon length **(C)**, and intron length **(D)** per gene among coding genes of giraffe, sheep, cattle, and human genomes are presented. The x-axes indicate lengths or numbers of genes, exons or introns, and y-axes represent their kernel densities. The similarities between these variables of our giraffe genome and published other mammal's genomes indicate that our assembly and annotation have high quality.

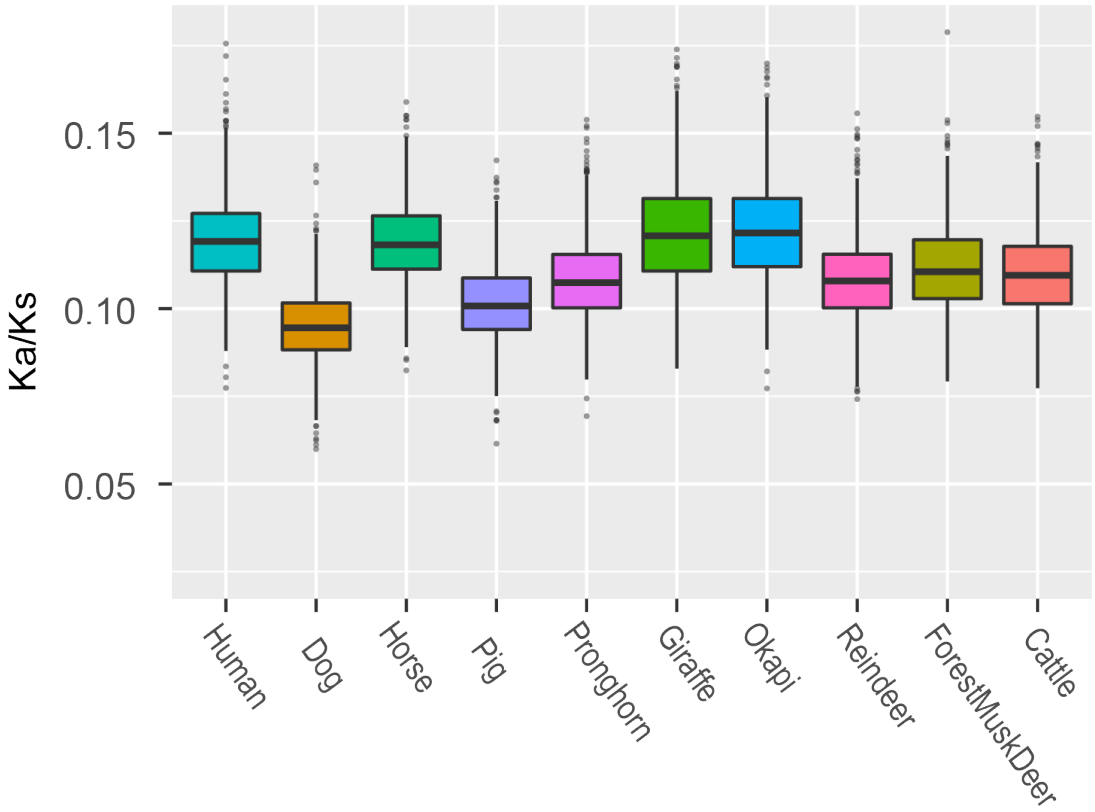

Fig. S7| The boxplot of Ka/Ks ratios across 10 species used for PAML analysis. For each species, the black line in the middle indicates the median value, while the lower and upper hinges correspond to the first and third quantiles (25^{th} and 75^{th} percentiles).

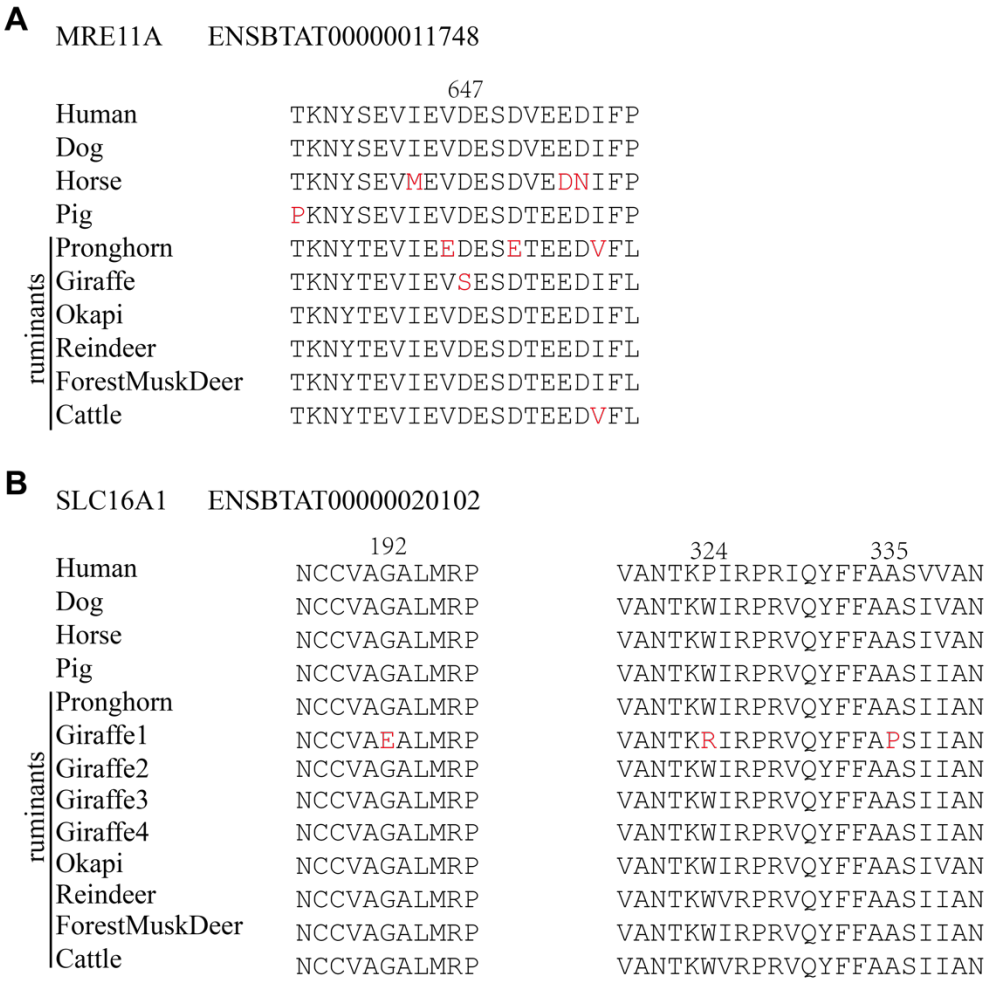

Fig. S8|Two false positive cases of the genes exhibiting adaptation in giraffe that have been reported by a previous study (*7*). (A) D647S was thought to be positively selected in giraffe before, although this substitution of giraffe is unique, in our data set with more ruminant clades, the nearby amino acids are not conserve in another ruminant clade, pronghorn, neither. **(B)** All the potential damaging substitutions reported before in SLC16A1, including G192E, W324R and A335P (Giraffe1, (*7*)), cannot be verified by any other giraffe genomes (Giraffe2, (*9*); Giraffe3, (*74*); Giraffe4, this study).

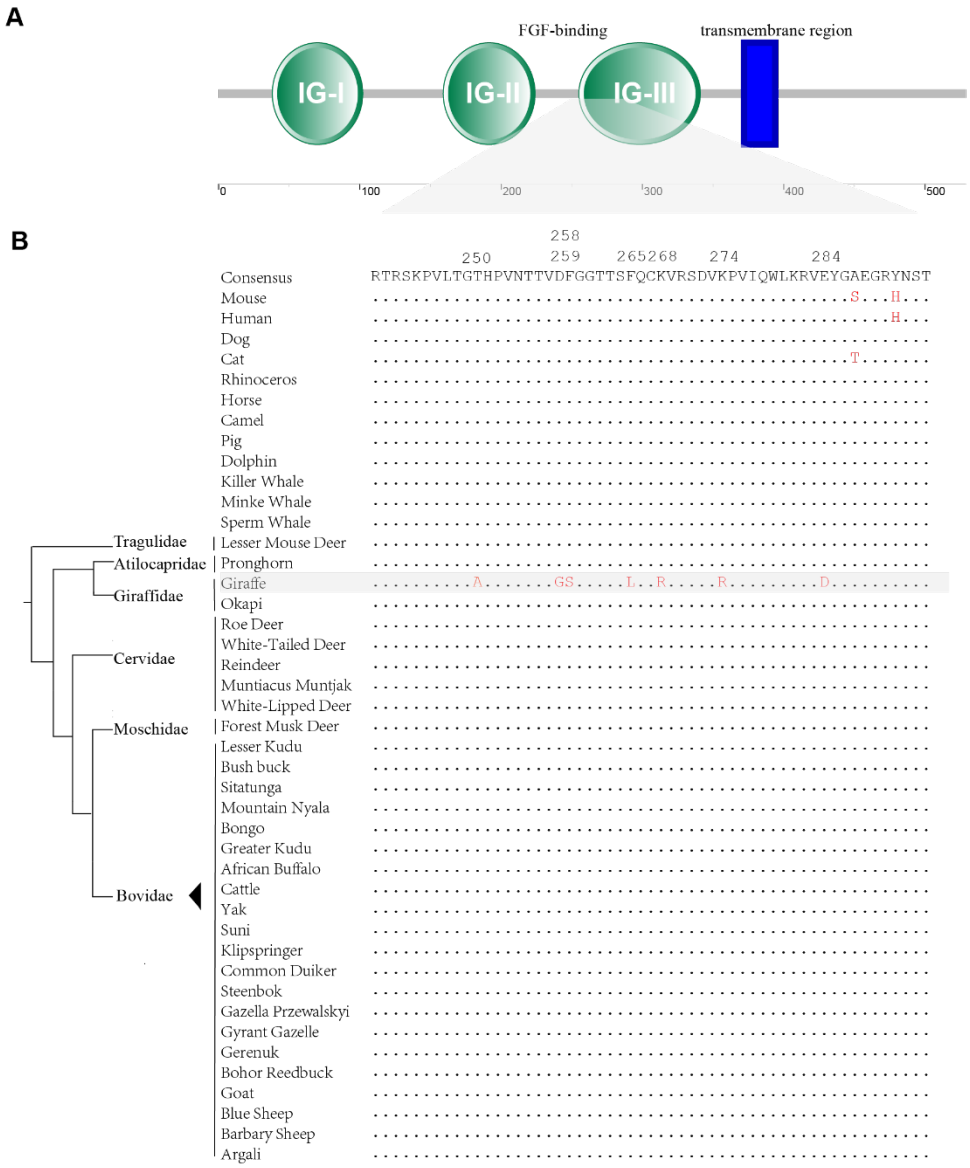

Fig. S9| Multi-sequence alignments of FGFRL1 proteins. (A) Functional domain annotation of giraffe FGFRL1 protein with online tool SMART(*75*) **(B)** Multi-sequence alignment around giraffe's seven unique substitutions in FGFRL1 among mammals, with all ruminant sequences in good quality showed. Common type amino acids are showed in first line of the alignment with following same sites showed as dots and different sites showed in red. There are seven unique substitutions in giraffe including T250A, D258G, F259S, F265L, K268R, K274 and E284D. And these variants have been verified by all available giraffe data sets by now (*7, 9, 56, 74*).

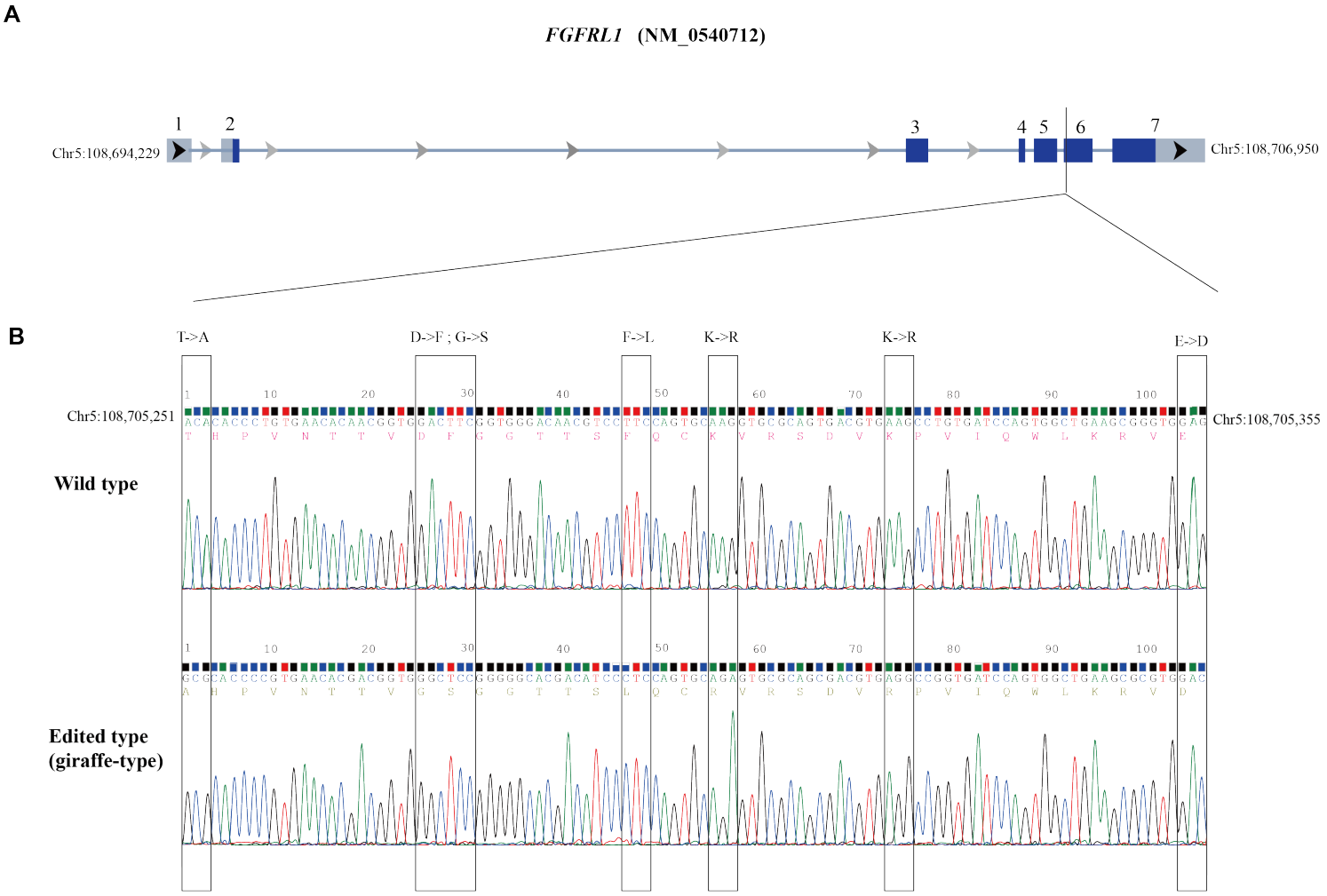

Fig. S10| Generation of *FGFRL1* edited homozygous mutant mice (C57). (A) Gene structure and location of *FGFRL1* in mice (GRCm38.p6). On exons, UTR regions are in light blue and CDS regions are in dark blue. The sites should be edited locate on the six exon. **(B)** PCR sequencing of the sites in edited type mice and wild type mice. It shows that all the seven sites in edited type mice have been changed to giraffe-type, and the all the sites are homozygous in both wild type and edited type mice.

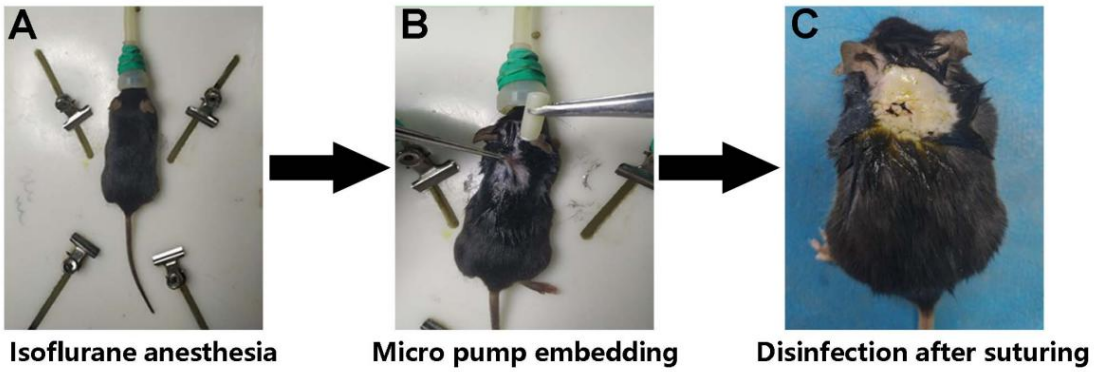

Fig. S11| Establishment of hypertension model in WT and giraffe-type *FGFRL1* mice. (A) Adult (16 weeks old, 24-26 g) WT (n=10) and giraffe-type *FGFRL1* mice (n=10) were immobilized and anesthetized with isoflurane (1% at 1.5 L/min oxygen). **(B)** A 1 cm incision on the back was then made by scissors and an Alzet-1004 osmotic mini-pump (Cupertino, CA) was embedded, providing Ang II (900 ng/kg/min at an infusion rate of 10 μl/hr) or equivalent saline. **(C)** The skin incision was sutured and disinfected. Photo Credit: Jianbo Gao, The Fourth Military Medical University.

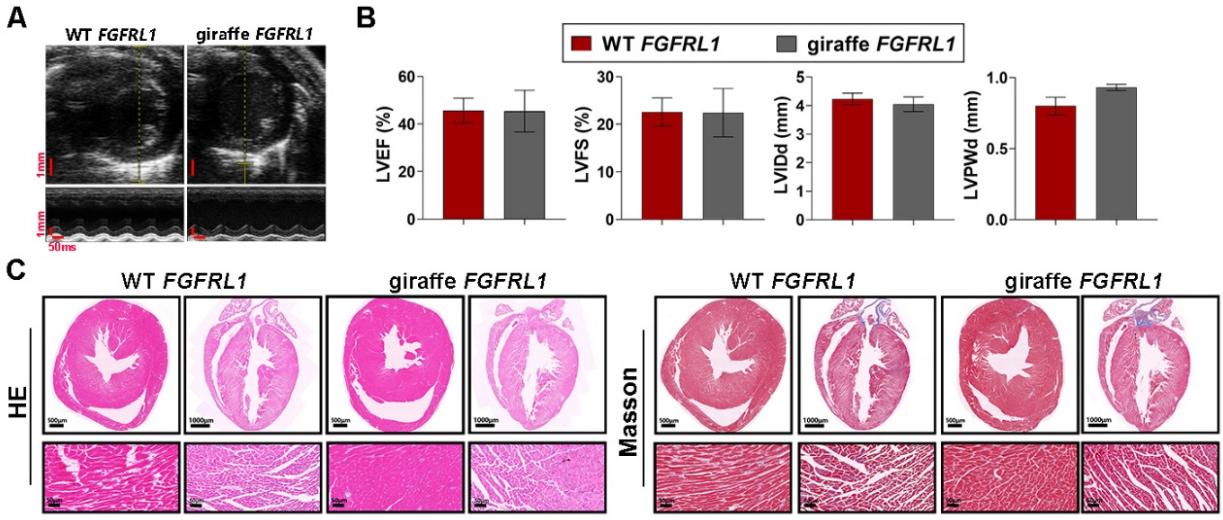

Fig. S12| No sign of defects was found in heart function and histology of giraffe-type *FGFRL1* mice. (A) Echocardiographic images of adult WT *FGFRL1* and giraffe-type *FGFRL1* mice. **(B)** No significant difference was found in left ventricular ejection fraction (LVEF), left ventricular fractional shortening (LVFS), left ventricular posterior wall thickness at end-diastole (LVPWd) and left ventricular internal diameter at end-diastole (LVIDd) between the WT *FGFRL1* and giraffe-type *FGFRL1* mice. n=4, $P>0.05$, independent Student's *t*-test. **(C)** No sign of defects in cardiac histology in adult giraffe-type *FGFRL1* mice were detected by HE and Masson trichrome staining either. Error bars indicate SD.

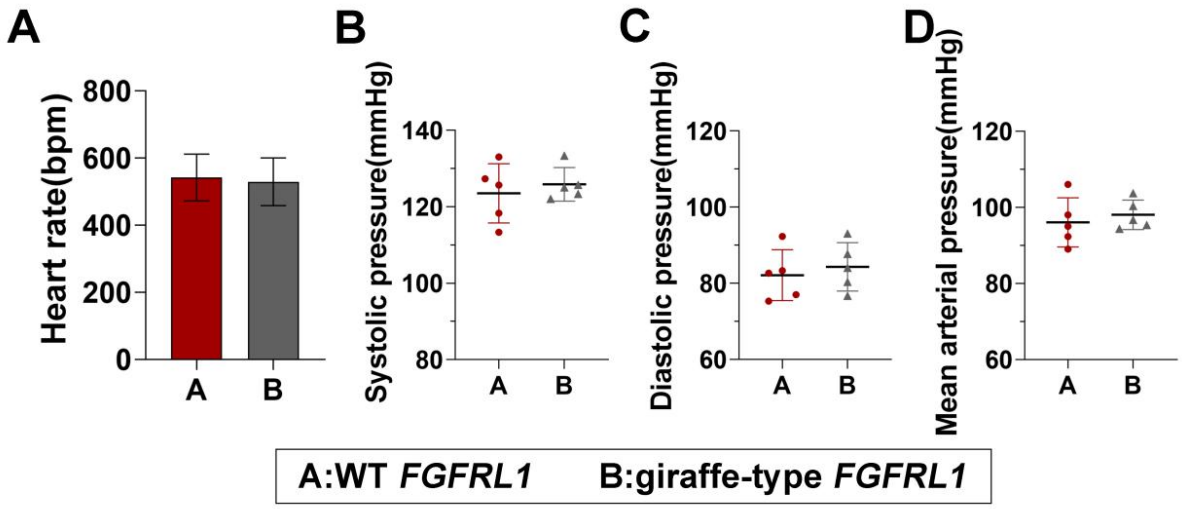

Fig. S13|Baseline heart rate and blood pressure in giraffe-type *FGFRL1* mice. No significant differences in baseline heart rate **(A)** or basal blood pressures **(B)**, systolic pressure; **(C)**, diastolic pressure; **(D)**, mean arterial pressure were detected between the adult giraffe-type *FGFRL1* mice and wild-type *FGFRL1* controls. n=5, $P>0.05$, independent Student's t-test. Error bars indicate SD.

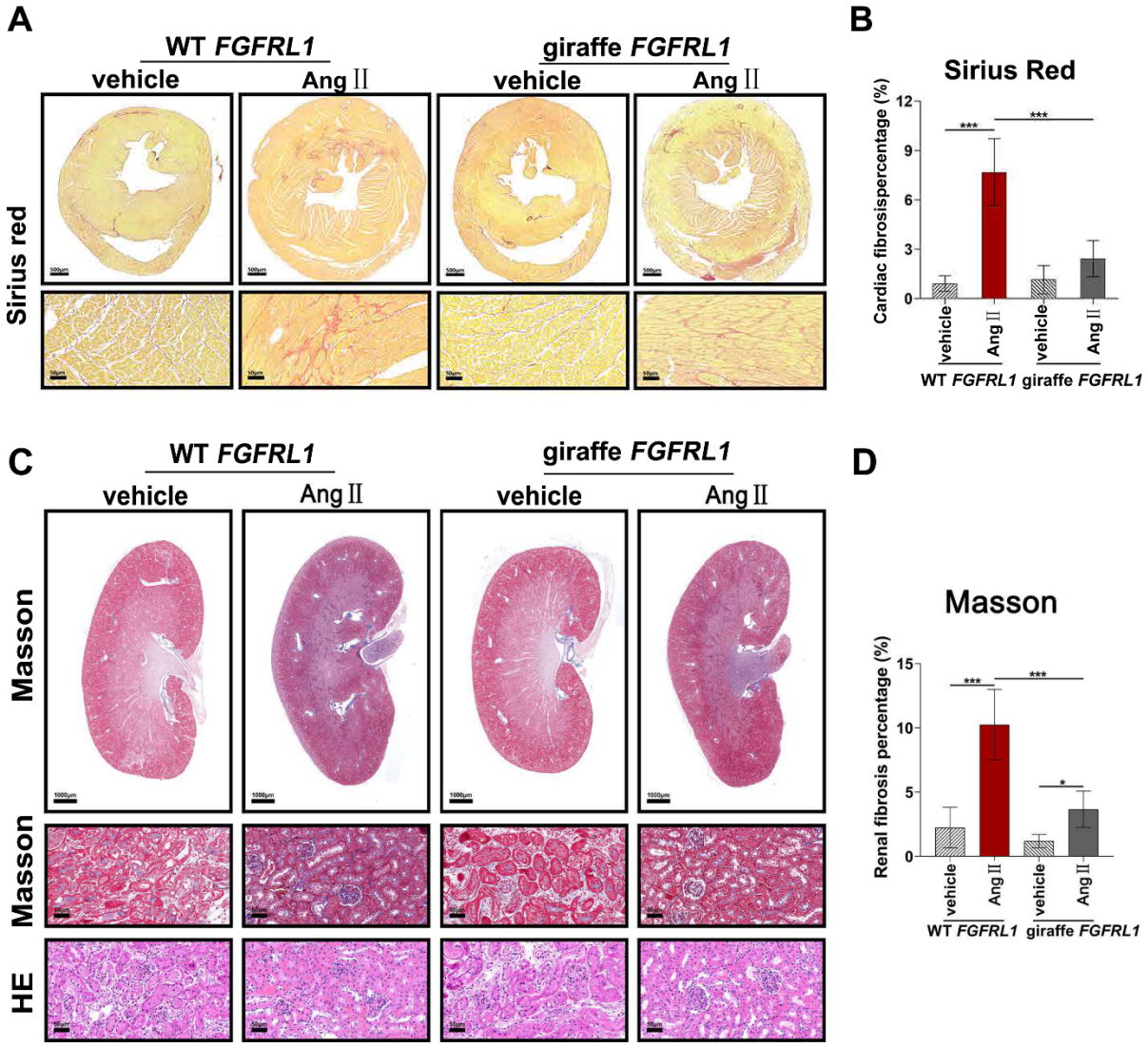

Fig. S14| Ang II-induced hypertension results in less myocardial and renal fibrosis in giraffe-type *FGFRL1* mice. (A) Representative histological images of Sirius Red-stained cross-sections of hearts of WT *FGFRL1* and giraffe-type *FGFRL1* mice infused for 28 days with vehicle or Ang II (900 ng/kg/min). **(B)** The proportion of collagen fibers (%) was significantly lower in giraffe-type *FGFRL1* mice than in the WT *FGFRL1* mice, when both were infused with Ang II for 28 days. n=6, ***$P<0.001$, one-way ANOVA followed by Tukey's post hoc test. Error bars indicate SD. **(C)** Representative histological images of Masson-stained and HE-stained cross-sections of kidney of WT *FGFRL1* and giraffe-type *FGFRL1* mice infused for 28 days with vehicle or Ang II (900 ng/kg/min). **(D)** The proportion of collagen fibers (%) was significantly lower in giraffe-type *FGFRL1* mice than in the WT *FGFRL1* mice, when both were infused with Ang II for 28 days. n=6, ***$P<0.001$, one-way ANOVA followed by Tukey's post hoc test. Error bars indicate SD.

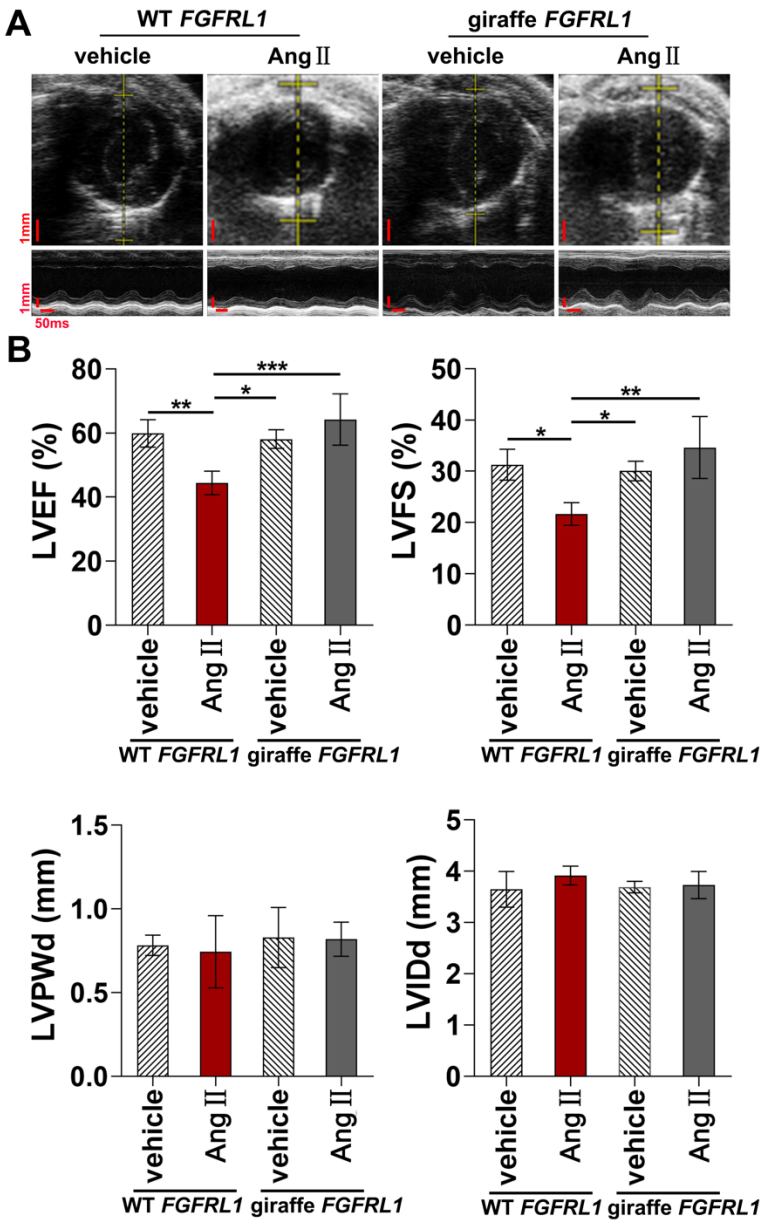

Fig. S15| Ang II-induced hypertension weakens myocardial function in WT *FGFRL1* mice. (A) Echocardiographic images of adult WT *FGFRL1* and giraffe-type *FGFRL1* mice, following infusion for 28 days with vehicle or Ang II (900 ng/kg/min). **(B)** Hypertension results in significant reductions in LVEF and LVFS, but not LVPWd and LVIDd, in WT *FGFRL1* mice after 28 days of Ang II infusion. The giraffe-type *FGFRL1* mice showed significantly higher LVEF and LVFS than the WT *FGFRL1* mice after 28 days of Ang II infusion. No significant difference was found in LVPWd or LVIDd between the giraffe-type *FGFRL1* mice and WT *FGFEL1* mice at the end of Ang II infusion. n=4, $*P<0.05$, $**P<0.01$, one-way ANOVA followed by Tukey's post hoc test. Error bars indicate SD.

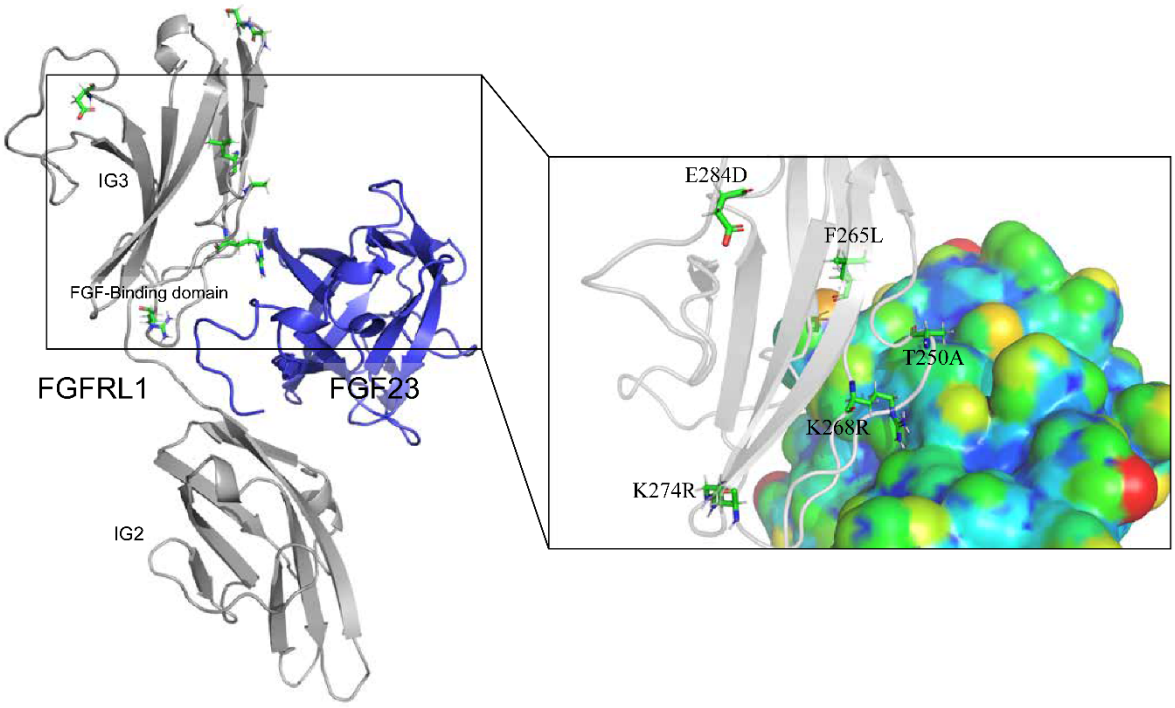

Fig. S16|3D modeling of the interaction between FGFRL1 and FGF23 proteins. 3D modeling showed that giraffe's seven unique substitutions (**Fig. S9**) (shown in green in the image to the left) are located near the FGF-binding and IG3 domain of FGFRL1. A close-up of the interaction interface is shown in the image to the right. According to the docking results, the interface score of mtFGFRL1 (-21.560 REU) is lower than that of wtFGFRL1 (-16.683 REU), and further MD simulation and MMGBSA calculation shows that the binding free energy of mtFGFRL1 (seven sites in giraffe-type) (-123.72 kj/mol ±1.24) is significantly lower than that of wtFGFRL1 (seven sites changed to common type) (-112.43 kj/mol ±0.79), which suggests that the mutation significantly enhance the binding affinity. Furthermore, the K268R mutation (shown to the right) is on part of the docking interface that contacts the polar surface of FGF23, and may significantly improve the interaction by enhancing polarity.

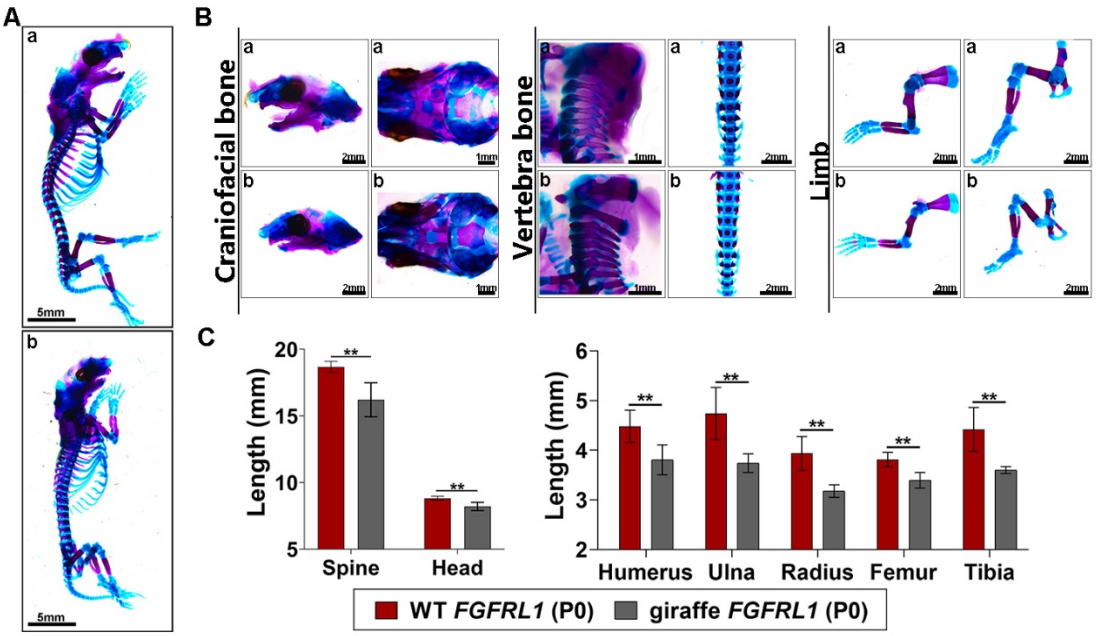

Fig. S17| Visualization of skeletons of P0 WT *FGFRL1* and giraffe-type *FGFRL1* mice stained with Alizarin red and Alcian blue. (A) Lateral view of whole-mount skeletons of P0 WT *FGFRL1* (a) and giraffe-type *FGFRL1* mice (b). **(B)** Representative images of craniofacial bone, vertebra bone and limbs in P0 WT *FGFRL1* (a) and giraffe-type *FGFRL1* mice (b). **(C)** The giraffe-type *FGFRL1* mice had significantly shorter heads, spines and limbs than WT *FGFRL1* mice. n=5, $^{**}P<0.01$, independent Student's *t*-test. Error bars indicate SD (standard deviations).

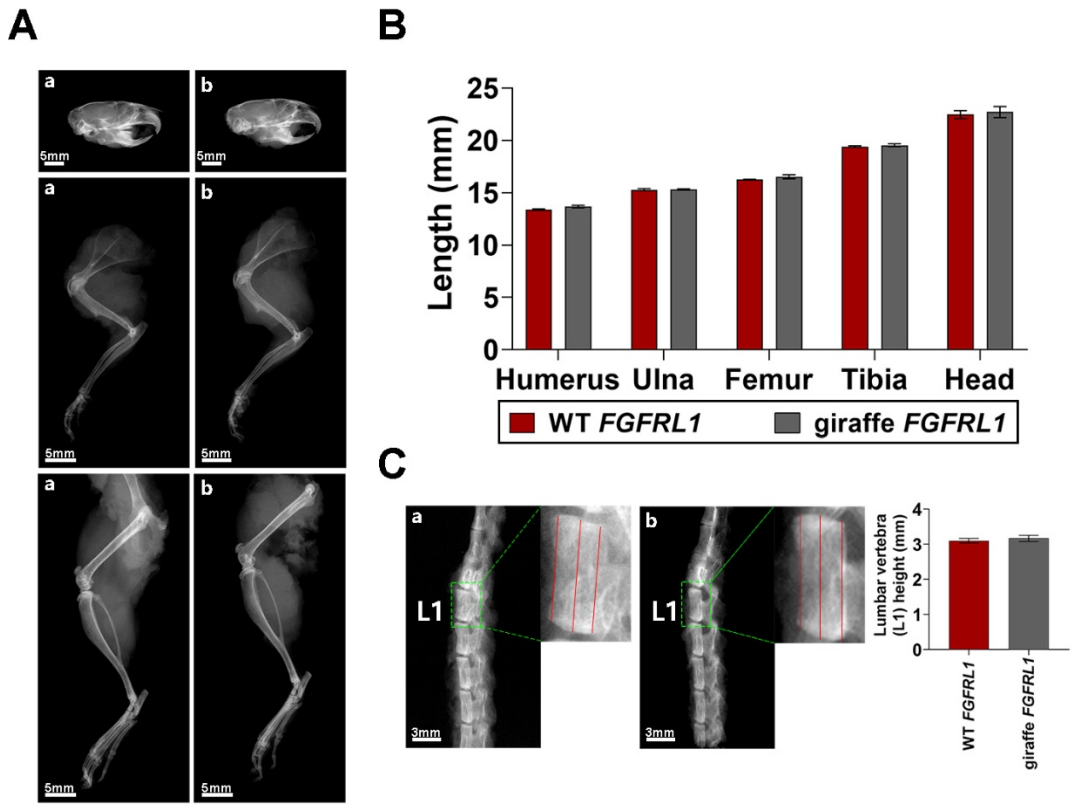

Fig. S18| Skeletal characteristics of adult WT *FGFRL1* and giraffe-type *FGFRL1* mice. (A) X-rays of skulls, forelimbs and hind limbs of adult WT *FGFRL1* (a) and giraffe-type *FGFRL1* mice (b). **(B)** No significant difference (n=3, p>0.05, independent Student's t-test) in limbs and head length was detected between adult WT *FGFRL1* and giraffe-type *FGFRL1* mice. **(C)** X-rays of the lumbar spine of adult WT *FGFRL1* (a) and giraffe-type *FGFRL1* mice (b). No significant difference (n=4, *P*>0.05, independent Student's t-test) in height of their L1 vertebra was found. Error bars indicate SD.

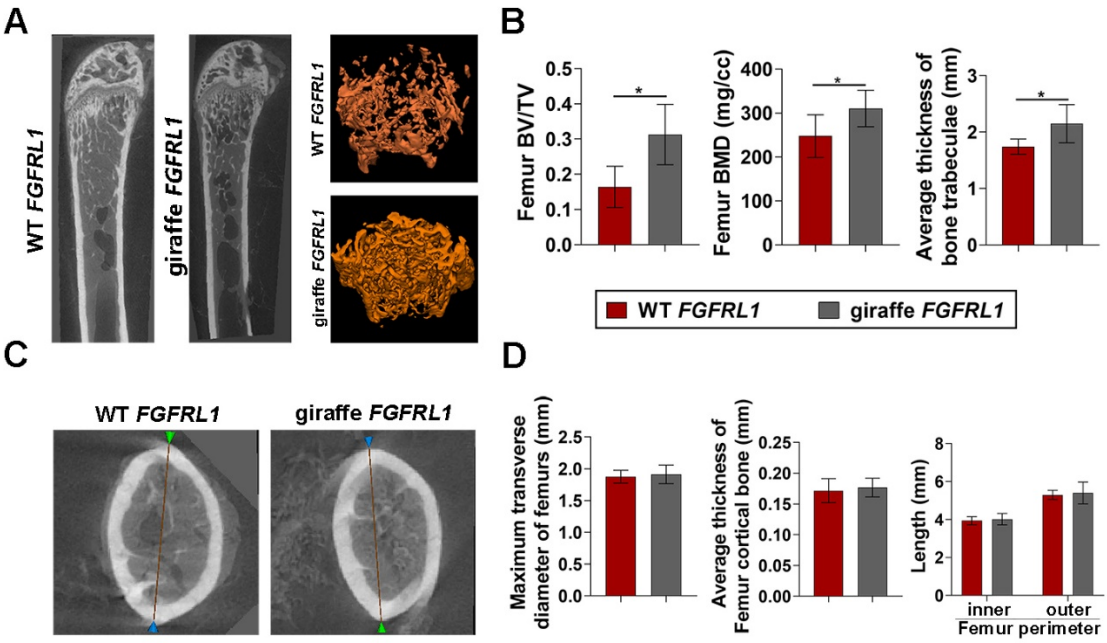

Fig. S19| Microstructural characteristics of distal femur in adult WT *FGFRL1* and giraffe-type *FGFRL1* mice. (A) Representative MicroCT images of distal femurs from the adult WT *FGFRL1* and giraffe-type *FGFRL1* mice. **(B)** The giraffe-type *FGFRL1* mice had significantly higher BMD, BV/TV and average trabeculae thickness in femurs than the WT *FGFRL1* mice. n=6, **P*＜0.05, independent Student's *t*-test. **(C)** MicroCT-derived images of the cortex at mid-diaphysis of femurs of adult WT *FGFRL1* and giraffe-type *FGFRL1* mice. **(D)** No significant difference was found in the maximum transverse diameter, average thickness of cortical bone, or inner and outer perimeter of femurs between the WT *FGFRL1* and giraffe-type *FGFRL1* mice. n=6, *P*>0.05, independent Student's *t*-test. Error bars indicate SD.

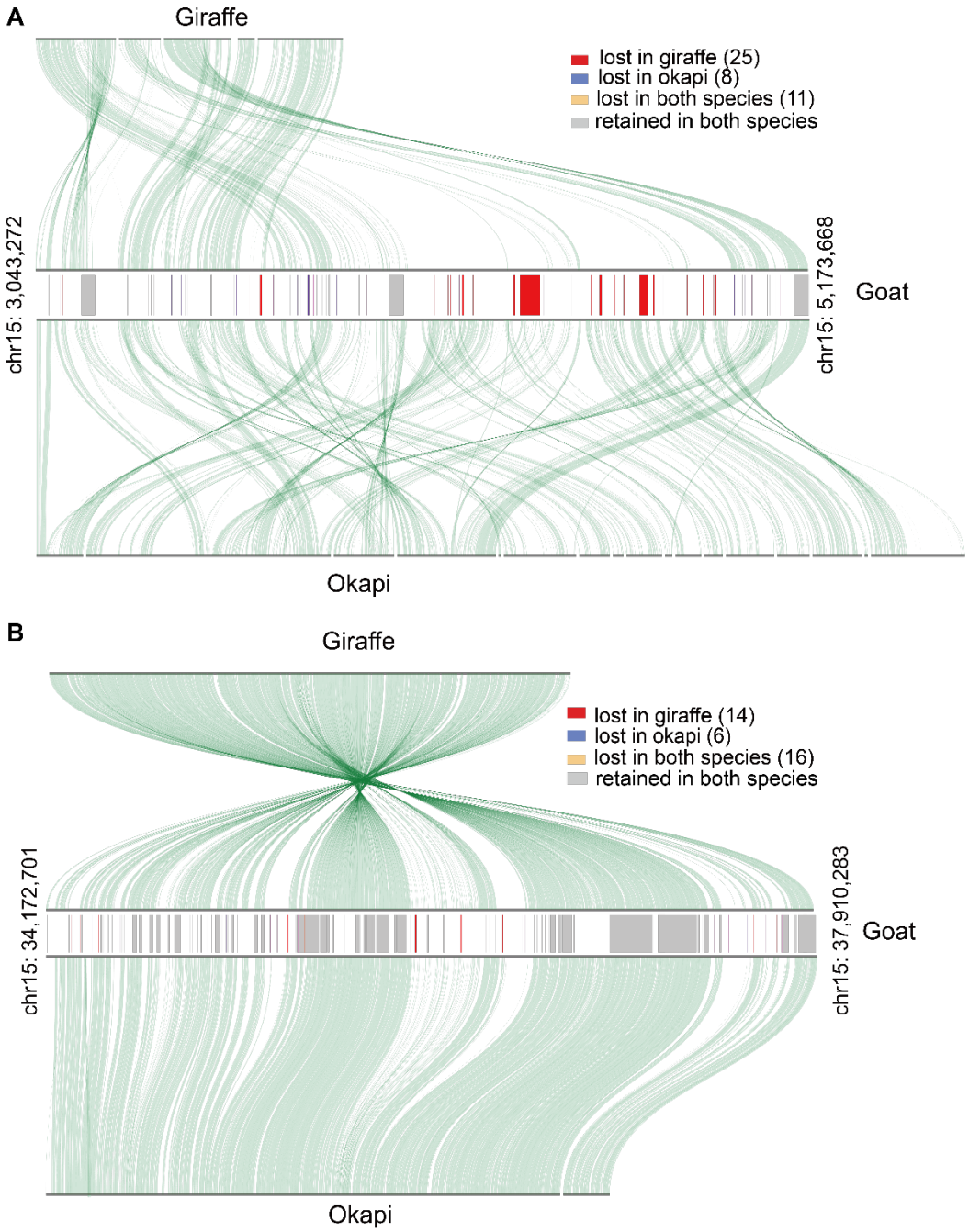

Fig. S20| Clusters of lost olfactory receptors (ORs) in the giraffe genome. With goat chromosome 15 as reference, the ORs uniquely lost in giraffe clustered in two regions, as shown in **(A)** and **(B)**. Within each region, positions of genes are shown as bars in the middle panel, and the alignments between giraffe-goat or okapi-goat are shown in the upper and lower panel respectively. In both regions, giraffe has lost more genes than okapi.

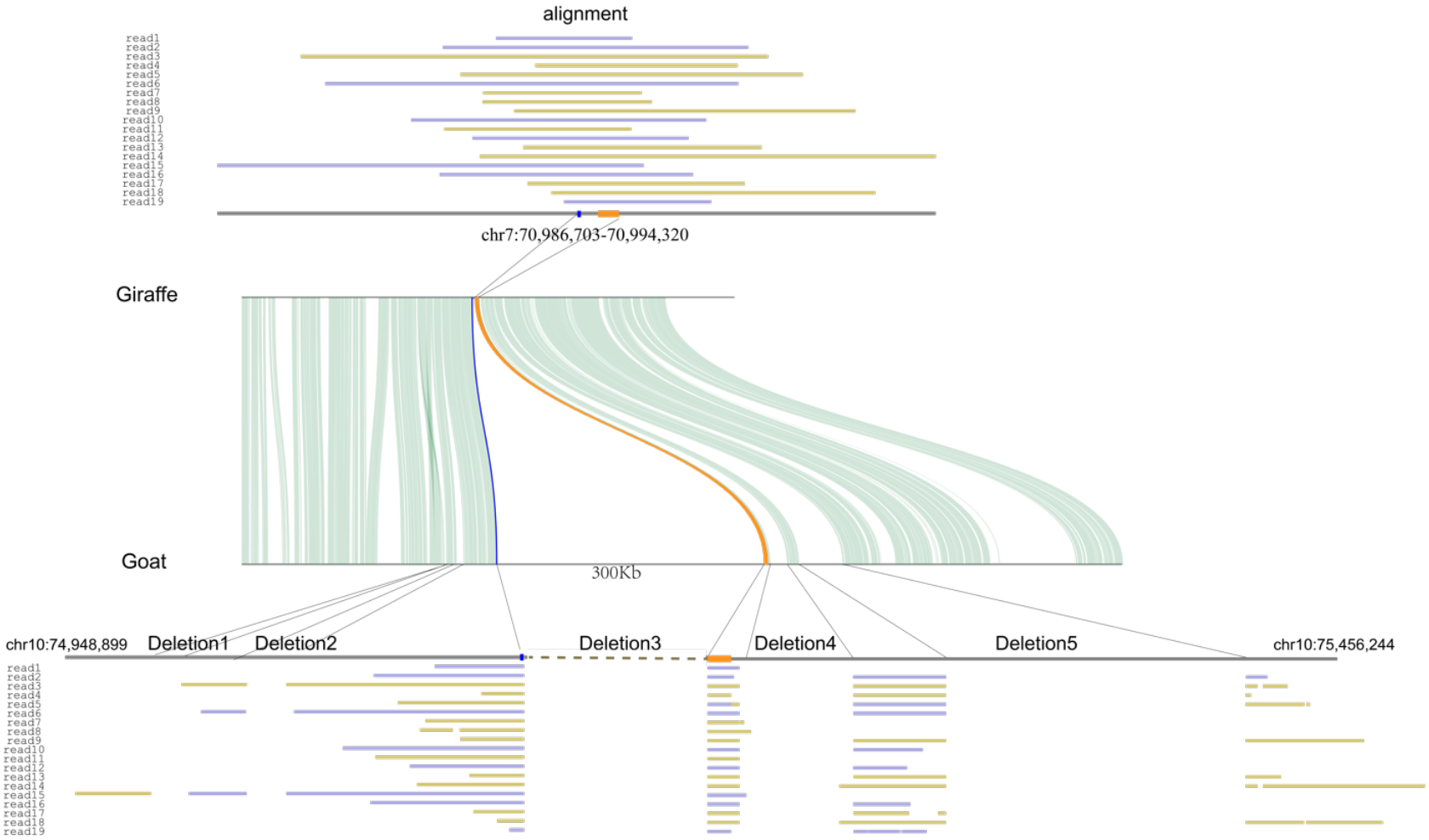

Fig. S21| Nanopore long reads of giraffe can finely span the deletion region in giraffe genome. With the largest deletion on giraffe's chr7 as an example (region Deletion3 on goat), 19 giraffe's long reads can finely span an 8kb region around the deletion (upper panel), however, these reads would be mapped to segmented regions on goat genome (ARS1) with other nearby deletion regions (Deletion1, 2, 4 and 5) cannot be mapped neither, which can help to rule out potential assembly error. The two synteny blocks nearby the largest deletion in giraffe were marked in blue or orange, and the color of reads represents mapping orientation.

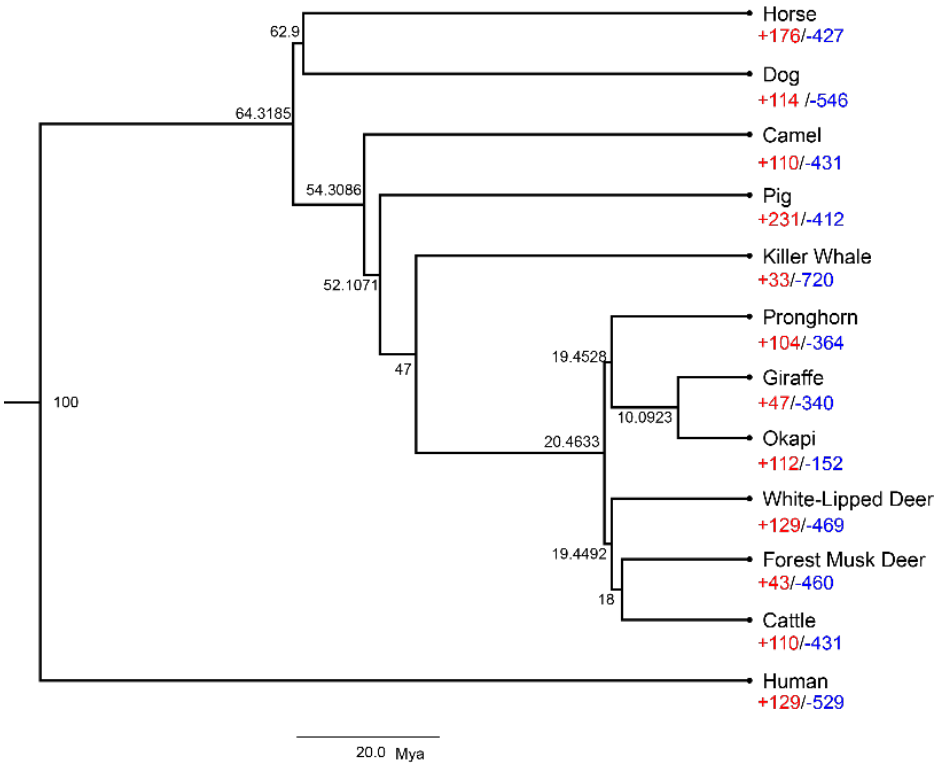

Fig. S22| Estimation of gene family expansion and contraction in giraffe and other mammals. Numbers of expanded and contracted gene families are shown in red and blue, respectively. The time tree used for CAFÉ analysis here was extracted from the ruminant study before (*9*).

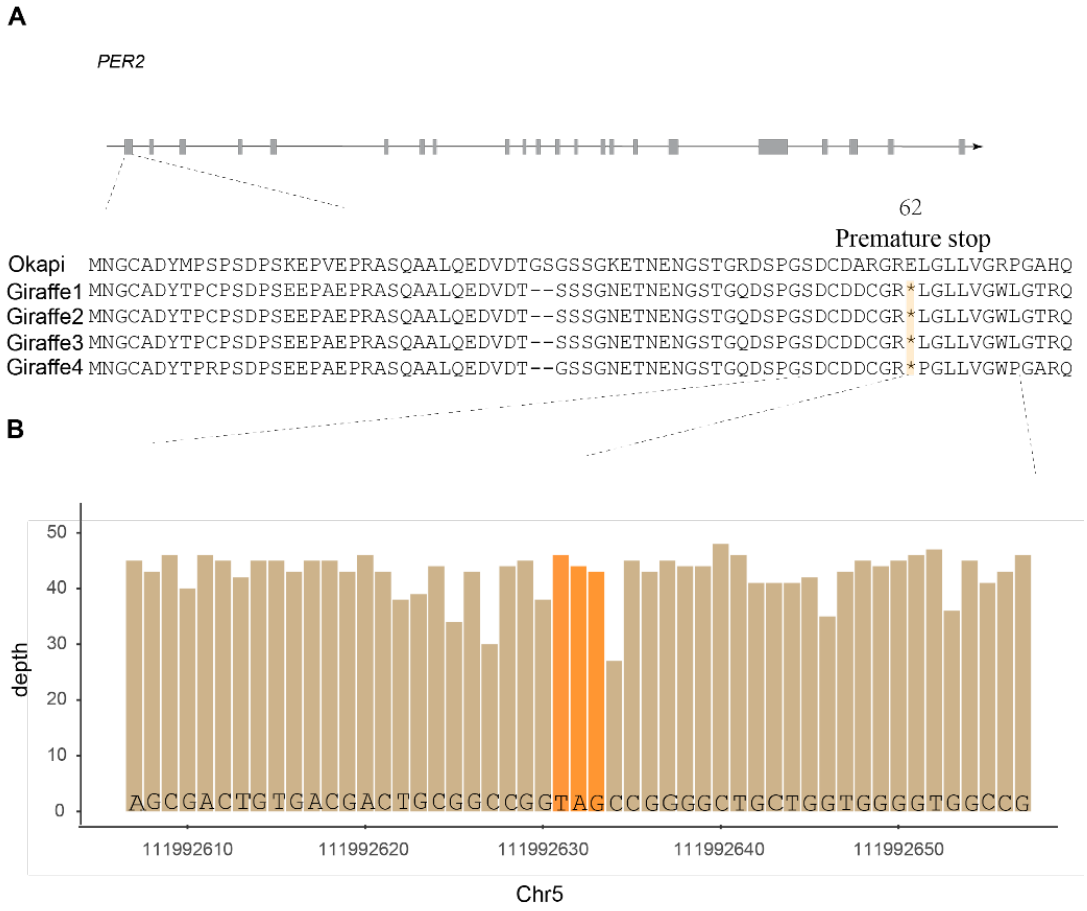

Fig. S23| A premature stop codon located in the first exon of *PER2*. (A) The gene structure of *PER2*, and the stop codon was verified by examination of currently available giraffe assemblies (Giraffe1: Agaba, M. et al (*7*); Giraffe2: Chen, L. et al (*9*); Giraffe3: Farre, M. et al (*74*); Giraffe4: this study). **(B)** Reads depth of the stop codon is similar as local region (genome average: 54×).

Table S1| Statistics summary of filtered sequencing data for genome assembly.

Type	Platform	Total reads	Total bases (Gb)	Depth (×)	Application
Third-generation	Nanopore	4,124,698	140.56	56	Assembly of initial contigs
Next generation	HiSeq2000	650,983,031	199.46	80	Genome survey and genomic base correction
HiC	HiSeq X Ten	693,531,404	138.71	55	Chromosome construction

The sequencing depth was calculated by the assembled genome size (Table S3)

Table S2| Quality statistics of the assembled giraffe genome.

Statistics	Contig		Scaffold	
	Length (bp)	Number	Length (bp)	Number
N90	6,097,037	74	118,944,183	13
N80	14,553,272	49	138,611,967	11
N70	21,216,402	36	153,209,366	10
N60	26,459,807	26	154,917,489	8
N50	35,949,831	19	158,234,173	7
Average length	2,827,641		1,164,272	
Max length	3,643,417		236,005,560	
Total length	2,400,667,334		2,441,480,433	
Total number	849		2,096	
Number >= 10 Kb	695		466	

Table S3| Summary statistics of assembled chromosome-level giraffe genome.

Chromosome	Length (bp)
1	210,418,314
2	235,793,497
3	188,969,416
4	210,259,023
5	186,608,127
6	176,660,016
7	154,882,256
8	153,136,160
9	153,708,084
10	158,058,458
11	133,580,009
12	137,671,694
13	118,918,659
14	56,087,642
X	114,100,299
Bases anchored to chromosomes	2,391,484,175
Unanchored scaffolds	2,081
Unanchored bases	49,996,258
Total length of genome	2,441,480,433
Chromosome/total	97.95%

Table S4| Mapping ratio of Nanopore reads to giraffe genome statistics.

Term	Reads number	Percentage (%)
MQ>=0	4,122,883	99.96
MQ>=5	4,102,423	99.46
MQ>=10	4,097,461	99.34
MQ>=30	4,079,596	98.91
MQ>=60	4,048,745	98.16
Total	4,124,698	--

MQ: Mapping quality, generated by minimap2 (*76*)

Table S5| Mapping ratio of Illumina reads to giraffe genome.

Library Type	Total reads	Mapped reads	Mapped reads ratio	Properly paired	Properly paired ratio
Illumina HiSeq2000	1,306,890,991	1,300,467,032	99.51%	1,264,730,380	97.14%

Table S6| Quality evaluation of the assembled genome and annotated protein set using BUSCO (v2.0)(*46*) software with "mammalia_odb9" dataset.

	Genome		Protein	
Types of BUSCOs	**Count**	**Ratio (%)**	**Count**	**Ratio (%)**
Complete BUSCOs	3,946	96.15	3,973	96.81
Complete and single-copy BUSCOs	3,829	93.30	3,922	95.57
Complete and duplicated BUSCOs	117	2.85	51	2.49
Fragmented BUSCOs	71	1.73	66	1.61
Missing BUSCOs	87	2.12	65	1.58

Table S7| Genome quality comparison of all available giraffe genomes.

Genome	Sequencing method	Chromosome	Genome BUSCO	Genome size (contigs>=500bp)	N ratio
Giraffe1(*7*)	Illumina	no	87.10%	2,593,494,537	3.63%
Giraffe2(*9*)	Illumina	no	94.90%	2,460,243,901	3.12%
Giraffe3(*74*)	Illumina + Chicago library	Yes (n=24)	95.00%	2,463,443,901	3.25%
Giraffe4 (This study)	Nanopore + Illumina + HiC	Yes (n=15)	96.15%	2,441,480,433	0.14%

Table S8| Repeat elements annotation of the giraffe genome.

Type	Repeat Size (bp)	Percent of genome (%)
Trf	41,261,019	1.69
Repeatmasker	889,431,322	36.43
Proteinmask	364,513,029	14.93
De novo	781,029,591	31.99
Total	1,056,916,879	43.29

Table S9| Statistics of transposable elements in giraffe genome.

	Repbase TEs		TE proteins		De novo		Combined TEs	
Type	Length (bp)	Percentage of genome(%)	Length (bp)	Percentage of genome(%)	Length (bp)	Percentage of genome(%)	Length (bp)	Percentage of genome(%)
DNA	46,876,424	1.92	6,591,997	0.27	34,180,726	1.40	57,130,642	2.34
LINE	563,981,980	23.10	349,131,702	14.30	567,644,201	23.25	739,768,571	30.30
SINE	175,786,591	7.20	0	0	23,926,508	0.98	177,739,776	7.28
LTR	112,308,100	4.60	9,033,478	0.37	69,826,340	2.86	119,632,541	4.90
Other	0	0	0	0	0	0	0	0
Unknown	488,296	0.02	0	0	105,960,251	4.34	106,204,399	4.35
Total	889,431,322	36.43	364,513,029	14.93	777,611,518	31.85	1,033,478,667	42.33

Table S10| Statistics of annotated genes from the *de novo*, homolog and final gene sets.

Methods		Total number	Average gene length (bp)	Average CDS length (bp)	Average exon number	Average exon length (bp)	Average intron length (bp)
De novo	Augustus	19,892	46,470.64	1,482.66	8.95	165.68	5,659.49
	Genscan	40,114	39,802.84	1,275.12	7.85	162.36	5,621.33
Homolog	Human	14,863	32,361.11	1,739.66	10.1	172.22	3,364.58
	Cattle	15,099	29,711.27	1,685.51	9.96	169.22	3,127.76
	Sheep	15,244	30,359.82	1,659.88	10.01	165.79	3,184.61
EVM	Giraffe	21,580	46,349.67	1,591.83	9.65	164.91	5,172.65

Table S11| Functional annotation of giraffe genes.

Database	Number	Percentage (%)
InterPro	16,875	78.19
GO	12,906	59.80
KEGG	14561	67.47
Swissprot	18,186	84.27
COG	6,909	32.02
TrEMBL	18,463	85.56
NR	16,767	77.70
Unannotated	2,959	13.71
Annotated	18,621	86.29
Total	21,580	

Table S12| Lengths of reconstructed ancestral chromosome (chr) karyotypes of Giraffidae and Bovidae.

Ancestral chr ID	Length (bp)	Ancestral chr ID	Length (bp)
1	145,495,223	16	66,435,077
2	128,455,352	17	66,132,375
3	112,730,851	18	65,762,662
4	108,139,951	19	64,478,890
5	107,405,570	20	59,548,638
6	107,307,673	21	58,379,626
7	99,033,524	22	57,917,096
8	93,818,976	23	54,207,695
9	91,582,586	24	49,215,121
10	89,219,325	25	47,378,180
11	87,492,783	26	46,476,476
12	84,212,973	27	43,894,601
13	80,597,291	28	41,155,042
14	75,694,660	29	20,592,860
15	74,210,038	30	18,933,069

Table S13| 101 PSGs identified in giraffe genome. The "Gene ID" column represents the gene ids of cattle (*Bos taurus*). In the "Gene symbol" column, * marked genes have been reported as PSGs in previous study, and # marked genes are those overlap with other highly divergent genes reported in previous study (*7*).

Gene ID	Gene symbol	Description	*p*-value	*q*-value
ENSBTAG00000014760	FOXE1	forkhead box E1	1.79E-06	5.63E-03
ENSBTAG00000013346	SIX5	SIX homeobox 5	2.13E-06	5.63E-03
ENSBTAG00000027464	FGFRL1*	fibroblast growth factor receptor-like 1	2.58E-06	5.68E-03
ENSBTAG00000012945	PDE6A	phosphodiesterase 6A	9.97E-05	1.14E-01
ENSBTAG00000000581	DOCK10	dedicator of cytokinesis 10	1.03E-04	1.14E-01
ENSBTAG00000012659	LRIF1	ligand dependent nuclear receptor interacting factor 1	2.31E-04	2.26E-01
ENSBTAG00000017425	GJB2	gap junction protein beta 2	3.75E-04	3.09E-01
ENSBTAG00000020856	HFM1	HFM1, ATP dependent DNA helicase homolog	6.57E-04	3.95E-01
ENSBTAG00000004322	FOS	Fos proto-oncogene, AP-1 transcription factor subunit	6.62E-04	3.95E-01
ENSBTAG00000025182	FBXL21	F-box and leucine rich repeat protein 21	8.35E-04	4.59E-01
ENSBTAG00000019139	PHF3	PHD finger protein 3	9.74E-04	4.94E-01
ENSBTAG00000010204	PCMT1	protein-L-isoaspartate (D-aspartate) O-methyltransferase	1.43E-03	6.51E-01
ENSBTAG00000004147	FBXO18	F-box protein, helicase, 18	1.62E-03	6.73E-01
ENSBTAG00000004722	THUMPD2	THUMP domain containing 2	1.67E-03	6.73E-01
ENSBTAG00000009085	SLC35A5	solute carrier family 35 member A5	1.68E-03	6.73E-01
ENSBTAG00000019565	NCOA4	nuclear receptor coactivator 4	2.11E-03	8.19E-01
ENSBTAG00000026307	ZNF629	zinc finger protein 629	2.40E-03	8.92E-01
ENSBTAG00000030864	FAM228B	family with sequence similarity 228 member B	2.43E-03	8.92E-01
ENSBTAG00000017852	ALDH9A1	aldehyde dehydrogenase 9 family member A1	2.65E-03	9.40E-01
ENSBTAG00000013955	TRAPPC9	trafficking protein particle complex 9	3.13E-03	1.00E+00
ENSBTAG00000005989	LAP3	leucine aminopeptidase 3	3.24E-03	1.00E+00
ENSBTAG00000011446	SEMA7A*	semaphorin 7A (John Milton Hagen blood group)	3.34E-03	1.00E+00
ENSBTAG00000020281	NIN	ninein	3.52E-03	1.00E+00
ENSBTAG00000033835	MPZ	myelin protein zero	3.91E-03	1.00E+00
ENSBTAG00000039582	NDUFC1	NADH:ubiquinone oxidoreductase subunit C1	4.18E-03	1.00E+00
ENSBTAG00000038600	LRRC15	leucine rich repeat containing 15	4.19E-03	1.00E+00
ENSBTAG00000038138	ACE3	angiotensin I converting enzyme (peptidyl-dipeptidase A) 3	4.48E-03	1.00E+00
ENSBTAG00000006404	CENPT	centromere protein T	4.78E-03	1.00E+00
ENSBTAG00000019843	HAUS6*	HAUS augmin like complex subunit 6	4.92E-03	1.00E+00

ENSBTAG00000009208	TCTN1	tectonic family member 1	5.07E-03	1.00E+00
ENSBTAG00000031765	CCDC189	coiled-coil domain containing 189	5.13E-03	1.00E+00
ENSBTAG00000013931	FAM96B	family with sequence similarity 96 member B	5.38E-03	1.00E+00
ENSBTAG00000020412	RAP2A	RAP2A, member of RAS oncogene family	5.42E-03	1.00E+00
ENSBTAG00000021971	SNCAIP	synuclein alpha interacting protein	5.58E-03	1.00E+00
ENSBTAG00000010775	POGK	pogo transposable element with KRAB domain	5.76E-03	1.00E+00
ENSBTAG00000038520	TMPRSS11E	NA	5.91E-03	1.00E+00
ENSBTAG00000011213	NTRK3	NA	6.95E-03	1.00E+00
ENSBTAG00000009254	CCDC129	coiled-coil domain containing 129	6.97E-03	1.00E+00
ENSBTAG00000011179	PDCD2	programmed cell death 2	7.12E-03	1.00E+00
ENSBTAG00000047087	MCIDAS	multiciliate differentiation and DNA synthesis associated cell cycle protein	8.05E-03	1.00E+00
ENSBTAG00000000542	CFAP36	cilia and flagella associated protein 36	8.48E-03	1.00E+00
ENSBTAG00000010719	ANGPTL1	angiopoietin like 1	8.52E-03	1.00E+00
ENSBTAG00000011876	MORC3	MORC family CW-type zinc finger 3	9.85E-03	1.00E+00
ENSBTAG00000031632	ADRA1A*	adrenoceptor alpha 1A	9.93E-03	1.00E+00
ENSBTAG00000001844	MOGS	mannosyl-oligosaccharide glucosidase	1.01E-02	1.00E+00
ENSBTAG00000014166	POLR1B	RNA polymerase I subunit B	1.02E-02	1.00E+00
ENSBTAG00000017517	ZNF236	zinc finger protein 236	1.02E-02	1.00E+00
ENSBTAG00000005477	LAPTM5	lysosomal protein transmembrane 5	1.03E-02	1.00E+00
ENSBTAG00000004782	PTPRCAP	protein tyrosine phosphatase, receptor type C associated protein	1.05E-02	1.00E+00
ENSBTAG00000006392	TTC7B	tetratricopeptide repeat domain 7B	1.22E-02	1.00E+00
ENSBTAG00000013380	CEP192	centrosomal protein 192	1.22E-02	1.00E+00
ENSBTAG00000016713	TMEM30B	transmembrane protein 30B	1.28E-02	1.00E+00
ENSBTAG00000019876	DSC1	desmocollin 1	1.34E-02	1.00E+00
ENSBTAG00000000326	ENTHD1	ENTH domain containing 1	1.35E-02	1.00E+00
ENSBTAG00000012519	XDH	xanthine dehydrogenase	1.41E-02	1.00E+00
ENSBTAG00000005016	AP3B1	adaptor related protein complex 3 beta 1 subunit	1.47E-02	1.00E+00
ENSBTAG00000003810	LOC524650	uncharacterized LOC524650	1.53E-02	1.00E+00
ENSBTAG00000000201	LTN1	listerin E3 ubiquitin protein ligase 1	1.55E-02	1.00E+00
ENSBTAG00000013283	PRR19*	proline rich 19	1.56E-02	1.00E+00
ENSBTAG00000011325	KHK	ketohexokinase	1.62E-02	1.00E+00
ENSBTAG00000007723	KDSR	3-ketodihydrosphingosine reductase	1.62E-02	1.00E+00
ENSBTAG00000015321	TRERF1	transcriptional regulating factor 1	1.67E-02	1.00E+00
ENSBTAG00000014158	CCNT2	cyclin T2	1.67E-02	1.00E+00

ENSBTAG00000018033	PIP4K2A	phosphatidylinositol-5-phosphate 4-kinase type 2 alpha	1.68E-02	1.00E+00
ENSBTAG00000012678	COLGALT1	collagen beta(1-O)galactosyltransferase 1	1.71E-02	1.00E+00
ENSBTAG00000010679	LRRC31	leucine rich repeat containing 31	1.78E-02	1.00E+00
ENSBTAG00000000888	SPTA1	spectrin alpha, erythrocytic 1	1.89E-02	1.00E+00
ENSBTAG00000026995	PNN	pinin, desmosome associated protein	1.91E-02	1.00E+00
ENSBTAG00000008322	KCNA10	potassium voltage-gated channel subfamily A member 10	1.94E-02	1.00E+00
ENSBTAG00000000219	GRIN2B	glutamate ionotropic receptor NMDA type subunit 2B	1.95E-02	1.00E+00
ENSBTAG00000014224	IGSF9B	immunoglobulin superfamily member 9B	1.97E-02	1.00E+00
ENSBTAG00000026986	TTN	titin	2.14E-02	1.00E+00
ENSBTAG00000005663	HAUS2#	HAUS augmin like complex subunit 2	2.21E-02	1.00E+00
ENSBTAG00000001138	UFSP1	UFM1 specific peptidase 1 (inactive)	2.25E-02	1.00E+00
ENSBTAG00000004364	THNSL2	threonine synthase like 2	2.30E-02	1.00E+00
ENSBTAG00000004494	B4GALNT1	beta-1,4-N-acetyl-galactosaminyltransferase 1	2.37E-02	1.00E+00
ENSBTAG00000020423	EP400	E1A binding protein p400	2.39E-02	1.00E+00
ENSBTAG00000012241	POLD2	DNA polymerase delta 2, accessory subunit	2.41E-02	1.00E+00
ENSBTAG00000037397	PRSS36	protease, serine 36	2.50E-02	1.00E+00
ENSBTAG00000048192	LOC100299320	putative olfactory receptor 10D4	2.50E-02	1.00E+00
ENSBTAG00000016717	CEP68	centrosomal protein 68	2.67E-02	1.00E+00
ENSBTAG00000015449	PPEF2	NA	2.75E-02	1.00E+00
ENSBTAG00000010283	MRPL37	NA	2.86E-02	1.00E+00
ENSBTAG00000010241	UNC5D	unc-5 netrin receptor D	3.14E-02	1.00E+00
ENSBTAG00000038606	DRD5	dopamine receptor D5	3.15E-02	1.00E+00
ENSBTAG00000015350	PLIN1	perilipin 1	3.25E-02	1.00E+00
ENSBTAG00000010306	RXFP1	relaxin/insulin like family peptide receptor 1	3.47E-02	1.00E+00
ENSBTAG00000007190	THAP6	THAP domain containing 6	3.52E-02	1.00E+00
ENSBTAG00000010118	HAT1	histone acetyltransferase 1	3.81E-02	1.00E+00
ENSBTAG00000004347	ADGRF5	adhesion G protein-coupled receptor F5	3.95E-02	1.00E+00
ENSBTAG00000039823	KBTBD7	kelch repeat and BTB domain-containing protein 7	4.03E-02	1.00E+00
ENSBTAG00000003061	LAMA5	laminin subunit alpha 5	4.05E-02	1.00E+00
ENSBTAG00000006013	NT5DC3	5'-nucleotidase domain containing 3	4.10E-02	1.00E+00
ENSBTAG00000002201	NFXL1*	nuclear transcription factor, X-box binding like 1	4.37E-02	1.00E+00
ENSBTAG00000044061	FAXC	failed axon connections homolog	4.60E-02	1.00E+00
ENSBTAG00000043961	MPDZ	multiple PDZ domain crumbs cell polarity complex component	4.60E-02	1.00E+00
ENSBTAG00000020457	TGFB1*	transforming growth factor beta 1	4.65E-02	1.00E+00

ENSBTAG00000039662	RSC1A1	protein DDI1 homolog 2	4.65E-02	1.00E+00
ENSBTAG00000002826	CLSPN	claspin	4.71E-02	1.00E+00
ENSBTAG00000006659	TMEM116	transmembrane protein 116	4.78E-02	1.00E+00
ENSBTAG00000034192	KIAA2012	KIAA2012 ortholog	4.83E-02	1.00E+00

Table S14| 359 REGs identified in giraffe genome. The "Gene ID" column represents the gene ids of cattle (*Bos taurus*). In the "Gene symbol" column, * marked genes have been reported as PSGs in previous study, and # marked genes are those overlap with other highly divergent genes reported in previous study (*7*).

Gene ID	Gene symbol	Description	*p*-value	*q*-value
ENSBTAG00000021497	CDH23	cadherin related 23	1.50E-07	9.98E-05
ENSBTAG00000008117	SLC5A4	solute carrier family 5 member 4	6.99E-07	4.19E-04
ENSBTAG00000003889	PER1	period circadian clock 1	8.74E-06	3.49E-03
ENSBTAG00000031209	SLC22A4	solute carrier family 22 member 4	1.14E-05	4.42E-03
ENSBTAG00000009510	ADRA2B#	adrenoceptor alpha 2B	1.76E-05	6.60E-03
ENSBTAG00000013153	NF2#	neurofibromin 2	1.99E-05	7.20E-03
ENSBTAG00000004746	HELZ	NA	2.53E-05	8.66E-03
ENSBTAG00000045905	PCDH15	protocadherin related 15	2.77E-05	9.21E-03
ENSBTAG00000015438	RRBP1	NA	3.40E-05	1.07E-02
ENSBTAG00000011171	PIEZO2	piezo type mechanosensitive ion channel component 2	6.72E-05	1.83E-02
ENSBTAG00000003410	EFL1	elongation factor like GTPase 1	8.96E-05	2.28E-02
ENSBTAG00000039485	MEIOC	meiosis specific with coiled-coil domain	1.04E-04	2.48E-02
ENSBTAG00000033677	WDR90	WD repeat domain 90	1.47E-04	3.27E-02
ENSBTAG00000018318	DNAJB5	DnaJ heat shock protein family (Hsp40) member B5	1.55E-04	3.36E-02
ENSBTAG00000007662	HSPA5	NA	1.60E-04	3.36E-02
ENSBTAG00000025337	MYH13	myosin-13	1.60E-04	3.36E-02
ENSBTAG00000020957	FZD5	frizzled class receptor 5	1.82E-04	3.69E-02
ENSBTAG00000025642	RYR3	ryanodine receptor 3	2.63E-04	5.16E-02
ENSBTAG00000017529	CA8	carbonic anhydrase 8	2.86E-04	5.52E-02
ENSBTAG00000007916	FOXJ1	forkhead box J1	2.93E-04	5.56E-02
ENSBTAG00000012225	KPNA2	karyopherin subunit alpha 2	3.08E-04	5.77E-02
ENSBTAG00000008943	ZSCAN12	zinc finger and SCAN domain containing 12	3.83E-04	6.86E-02
ENSBTAG00000020209	TIGD7	NA	4.25E-04	7.44E-02
ENSBTAG00000002414	KCNJ10	potassium voltage-gated channel subfamily J member 10	4.29E-04	7.44E-02
ENSBTAG00000000745	AQP1	aquaporin 1 (Colton blood group)	4.41E-04	7.54E-02
ENSBTAG00000022169	PREX2	phosphatidylinositol-3,4,5-trisphosphate dependent Rac exchange factor 2	4.58E-04	7.73E-02
ENSBTAG00000001030	MTMR3	myotubularin related protein 3	4.75E-04	7.90E-02
ENSBTAG00000002253	FKBP6	FK506 binding protein 6	5.12E-04	8.40E-02

ENSBTAG00000027337	CTSA	cathepsin A	5.27E-04	8.52E-02
ENSBTAG00000022915	OR4Q2	olfactory receptor 4Q2	6.21E-04	9.73E-02
ENSBTAG00000003710	XPO4	exportin 4	6.32E-04	9.73E-02
ENSBTAG00000007817	BRCC3	BRCA1/BRCA2-containing complex subunit 3	8.37E-04	1.19E-01
ENSBTAG00000003191	FSCN1#	fascin actin-bundling protein 1	8.42E-04	1.19E-01
ENSBTAG00000020540	TMEM198	transmembrane protein 198	1.00E-03	1.38E-01
ENSBTAG00000006417	EDC4	enhancer of mRNA decapping 4	1.04E-03	1.42E-01
ENSBTAG00000002398	ZNF567	zinc finger protein 567	1.14E-03	1.43E-01
ENSBTAG00000017747	PLSCR3	phospholipid scramblase 3	1.15E-03	1.43E-01
ENSBTAG00000010478	AIP	aryl hydrocarbon receptor interacting protein	1.15E-03	1.43E-01
ENSBTAG00000007128	ATP13A1	ATPase 13A1	1.24E-03	1.53E-01
ENSBTAG00000046573	PGBD1	NA	1.25E-03	1.53E-01
ENSBTAG00000021195	A1CF	APOBEC1 complementation factor	1.32E-03	1.58E-01
ENSBTAG00000008025	UBE3C	ubiquitin protein ligase E3C	1.35E-03	1.59E-01
ENSBTAG00000024199	KMT2C	lysine methyltransferase 2C	1.37E-03	1.59E-01
ENSBTAG00000032591	CTHRC1	collagen triple helix repeat-containing protein 1	1.41E-03	1.59E-01
ENSBTAG00000045625	NTN3	netrin 3	1.43E-03	1.59E-01
ENSBTAG00000019883	IST1	IST1, ESCRT-III associated factor	1.46E-03	1.59E-01
ENSBTAG00000008057	PARVG	parvin gamma	1.50E-03	1.62E-01
ENSBTAG00000009166	GSX1	GS homeobox 1	1.69E-03	1.77E-01
ENSBTAG00000000595	FBN3	fibrillin 3	1.78E-03	1.86E-01
ENSBTAG00000044100	HEATR1	HEAT repeat containing 1	1.81E-03	1.87E-01
ENSBTAG00000020402	TDRD9	tudor domain containing 9	1.84E-03	1.88E-01
ENSBTAG00000019814	PGBD2	piggyBac transposable element derived 2	1.97E-03	1.95E-01
ENSBTAG00000001189	AP1B1	adaptor related protein complex 1 beta 1 subunit	2.09E-03	2.01E-01
ENSBTAG00000009267	UHRF1BP1	UHRF1 binding protein 1	2.09E-03	2.01E-01
ENSBTAG00000026523	PLAGL1	PLAG1 like zinc finger 1	2.28E-03	2.11E-01
ENSBTAG00000004604	CCDC124	coiled-coil domain containing 124	2.29E-03	2.11E-01
ENSBTAG00000016396	PDE11A	phosphodiesterase 11A	2.32E-03	2.12E-01
ENSBTAG00000017136	SSTR2#	somatostatin receptor 2	2.45E-03	2.19E-01
ENSBTAG00000003819	STK36	serine/threonine kinase 36	2.57E-03	2.25E-01
ENSBTAG00000004987	NUP210L	nucleoporin 210 like	2.61E-03	2.27E-01
ENSBTAG00000019946	USP44	ubiquitin specific peptidase 44	2.68E-03	2.31E-01
ENSBTAG00000009123	ING5	inhibitor of growth family member 5	2.91E-03	2.42E-01

ENSBTAG00000019337	ACVR1C	activin A receptor type 1C	3.23E-03	2.63E-01
ENSBTAG00000008142	IFIH1	interferon induced with helicase C domain 1	3.25E-03	2.63E-01
ENSBTAG00000019954	ABHD2#	abhydrolase domain containing 2	3.32E-03	2.67E-01
ENSBTAG00000001302	MRPS28	mitochondrial ribosomal protein S28	3.38E-03	2.68E-01
ENSBTAG00000037581	MZF1	myeloid zinc finger 1	3.46E-03	2.71E-01
ENSBTAG00000006507	ADAMTS3	ADAM metallopeptidase with thrombospondin type 1 motif 3	3.48E-03	2.71E-01
ENSBTAG00000020014	CEP104	centrosomal protein 104	3.51E-03	2.71E-01
ENSBTAG00000005148	PTX4	pentraxin 4	3.53E-03	2.71E-01
ENSBTAG00000014502	BRAT1	BRCA1 associated ATM activator 1	3.64E-03	2.78E-01
ENSBTAG00000007305	VPS41	VPS41, HOPS complex subunit	3.72E-03	2.82E-01
ENSBTAG00000018638	CC2D2A	coiled-coil and C2 domain containing 2A	3.85E-03	2.90E-01
ENSBTAG00000008180	SPDL1	spindle apparatus coiled-coil protein 1	3.91E-03	2.93E-01
ENSBTAG00000018637	HDDC3	HD domain containing 3	3.94E-03	2.93E-01
ENSBTAG00000013210	ADAMTS4	ADAM metallopeptidase with thrombospondin type 1 motif 4	4.23E-03	3.05E-01
ENSBTAG00000009852	NAV3	neuron navigator 3	4.40E-03	3.13E-01
ENSBTAG00000009994	EML5	echinoderm microtubule associated protein like 5	4.47E-03	3.15E-01
ENSBTAG00000006925	CENPL	centromere protein L	4.65E-03	3.24E-01
ENSBTAG00000020262	PSME4	proteasome activator subunit 4	4.74E-03	3.27E-01
ENSBTAG00000000382	MED27	mediator complex subunit 27	4.96E-03	3.27E-01
ENSBTAG00000017296	POLN	DNA polymerase nu	5.05E-03	3.28E-01
ENSBTAG00000014940	KCNAB3	potassium voltage-gated channel subfamily A regulatory beta subunit 3	5.07E-03	3.28E-01
ENSBTAG00000013204	ATP13A3	ATPase 13A3	5.11E-03	3.29E-01
ENSBTAG00000011516	LRP12	LDL receptor related protein 12	5.42E-03	3.43E-01
ENSBTAG00000003458	CDCA7	cell division cycle associated 7	5.67E-03	3.55E-01
ENSBTAG00000000959	ZSWIM1	zinc finger SWIM-type containing 1	5.74E-03	3.58E-01
ENSBTAG00000038869	ZNF383	zinc finger protein 383	5.80E-03	3.58E-01
ENSBTAG00000007584	INPP1	inositol polyphosphate-1-phosphatase	5.83E-03	3.58E-01
ENSBTAG00000014099	YTHDC2	YTH domain containing 2	5.89E-03	3.58E-01
ENSBTAG00000020296	UBR3	ubiquitin protein ligase E3 component n-recognin 3 (putative)	5.94E-03	3.58E-01
ENSBTAG00000013112	C7H5orf15	chromosome 7 open reading frame, human C5orf15	6.37E-03	3.78E-01
ENSBTAG00000002715	GMPR2	guanosine monophosphate reductase 2	6.50E-03	3.78E-01
ENSBTAG00000015180	ATP6AP2	NA	6.56E-03	3.78E-01
ENSBTAG00000004933	KLHDC2	kelch domain containing 2	6.59E-03	3.78E-01

ENSBTAG00000005522	PLSCR5	phospholipid scramblase family member 5	6.59E-03	3.78E-01
ENSBTAG00000015798	UCKL1	uridine-cytidine kinase 1 like 1	6.78E-03	3.85E-01
ENSBTAG00000007417	GDF11	growth differentiation factor 11	6.87E-03	3.88E-01
ENSBTAG00000045954	LRRC14B	leucine rich repeat containing 14B	6.94E-03	3.90E-01
ENSBTAG00000012605	GPR157	G protein-coupled receptor 157	7.00E-03	3.91E-01
ENSBTAG00000004540	NUB1	negative regulator of ubiquitin like proteins 1	7.05E-03	3.91E-01
ENSBTAG00000021336	KIF5A	kinesin family member 5A	7.22E-03	3.95E-01
ENSBTAG00000011950	EMC1	ER membrane protein complex subunit 1	7.37E-03	4.00E-01
ENSBTAG00000032089	CDC42EP2*	CDC42 effector protein 2	7.40E-03	4.00E-01
ENSBTAG00000015334	ZHX1	zinc fingers and homeoboxes 1	7.43E-03	4.00E-01
ENSBTAG00000015647	CYP4X1	cytochrome P450 4X1	7.45E-03	4.00E-01
ENSBTAG00000015385	CTDSPL2	CTD small phosphatase like 2	7.54E-03	4.00E-01
ENSBTAG00000011413	CCDC107	coiled-coil domain containing 107	7.74E-03	4.06E-01
ENSBTAG00000010427	RASSF5	Ras association domain family member 5	8.07E-03	4.17E-01
ENSBTAG00000031614	BOLL	boule homolog, RNA binding protein	8.10E-03	4.17E-01
ENSBTAG00000020160	RNF138	ring finger protein 138	8.12E-03	4.17E-01
ENSBTAG00000023018	PARG	poly(ADP-ribose) glycohydrolase	8.25E-03	4.22E-01
ENSBTAG00000001644	MDN1	midasin AAA ATPase 1	8.49E-03	4.32E-01
ENSBTAG00000027727	PDZPH1P	PDZ and pleckstrin homology domains 1, pseudogene	8.78E-03	4.39E-01
ENSBTAG00000009383	KIF11	kinesin family member 11	8.81E-03	4.39E-01
ENSBTAG00000010235	NOP9	NOP9 nucleolar protein	8.81E-03	4.39E-01
ENSBTAG00000046020	OR2F1;OR2F2	olfactory receptor-like protein OLF3	9.05E-03	4.41E-01
ENSBTAG00000003813	BCS1L	BCS1-like (S. cerevisiae)	9.07E-03	4.41E-01
ENSBTAG00000039328	PURG	NA	9.20E-03	4.41E-01
ENSBTAG00000000611	C25H16orf90	chromosome 25 open reading frame, human C16orf90	9.43E-03	4.44E-01
ENSBTAG00000017711	WHAMM	WAS protein homolog associated with actin, golgi membranes and microtubules	9.47E-03	4.44E-01
ENSBTAG00000009406	GPBP1L1	NA	9.49E-03	4.44E-01
ENSBTAG00000047868	TMOD3	NA	9.61E-03	4.44E-01
ENSBTAG00000016152	DAB2	DAB2, clathrin adaptor protein	9.70E-03	4.45E-01
ENSBTAG00000000665	HCRT	hypocretin neuropeptide precursor	9.77E-03	4.45E-01
ENSBTAG00000010998	CFLAR	CASP8 and FADD like apoptosis regulator	9.88E-03	4.48E-01
ENSBTAG00000007110	RCOR3	REST corepressor 3	1.01E-02	4.49E-01
ENSBTAG00000005300	TMEM51	transmembrane protein 51	1.01E-02	4.49E-01

ENSBTAG00000006447	ACSM3#	acyl-CoA synthetase medium-chain family member 3	1.01E-02	4.49E-01
ENSBTAG00000039677	OR2B6	olfactory receptor, family 2, subfamily B, member 6	1.01E-02	4.49E-01
ENSBTAG00000000859	SLC38A1	solute carrier family 38 member 1	1.05E-02	4.59E-01
ENSBTAG00000033041	YIPF4	Yip1 domain family member 4	1.05E-02	4.60E-01
ENSBTAG00000047670	CHST8	carbohydrate sulfotransferase 8	1.08E-02	4.67E-01
ENSBTAG00000019907	WNK4	WNK lysine deficient protein kinase 4	1.09E-02	4.67E-01
ENSBTAG00000030520	PROB1	proline rich basic protein 1	1.11E-02	4.74E-01
ENSBTAG00000003938	FNDC1	fibronectin type III domain-containing protein 1	1.12E-02	4.78E-01
ENSBTAG00000005293	CDC25C	cell division cycle 25C	1.12E-02	4.78E-01
ENSBTAG00000012086	CNOT8	CCR4-NOT transcription complex subunit 8	1.13E-02	4.78E-01
ENSBTAG00000046223	ANAPC2	anaphase promoting complex subunit 2	1.14E-02	4.80E-01
ENSBTAG00000015459	KCNA2	potassium voltage-gated channel subfamily A member 2	1.16E-02	4.86E-01
ENSBTAG00000002086	PRPF4B	pre-mRNA processing factor 4B	1.19E-02	4.88E-01
ENSBTAG00000026676	SDC3	syndecan 3	1.19E-02	4.88E-01
ENSBTAG00000008397	ZNF555	zinc finger protein 555	1.20E-02	4.88E-01
ENSBTAG00000002407	TDRD5	tudor domain containing 5	1.20E-02	4.88E-01
ENSBTAG00000021360	RASGEF1C	NA	1.20E-02	4.88E-01
ENSBTAG00000005207	COPS7B	COP9 signalosome subunit 7B	1.24E-02	4.97E-01
ENSBTAG00000011336	OTOGL	otogelin like	1.26E-02	5.01E-01
ENSBTAG00000047048	DNAJC21	NA	1.29E-02	5.09E-01
ENSBTAG00000023734	PARD6A	par-6 family cell polarity regulator alpha	1.30E-02	5.11E-01
ENSBTAG00000012144	ZMYND19	zinc finger MYND-type containing 19	1.32E-02	5.12E-01
ENSBTAG00000015230	PLA2G12A	phospholipase A2 group XIIA	1.33E-02	5.14E-01
ENSBTAG00000018904	ENKD1	enkurin domain containing 1	1.34E-02	5.14E-01
ENSBTAG00000046142	PRKAR1B	NA	1.36E-02	5.16E-01
ENSBTAG00000023611	ZBTB32	zinc finger and BTB domain containing 32	1.40E-02	5.26E-01
ENSBTAG00000018383	ATAD5	ATPase family, AAA domain containing 5	1.43E-02	5.26E-01
ENSBTAG00000011635	CENPN	centromere protein N	1.43E-02	5.26E-01
ENSBTAG00000012784	RACGAP1	Rac GTPase activating protein 1	1.43E-02	5.26E-01
ENSBTAG00000012753	BRF1	BRF1, RNA polymerase III transcription initiation factor 90 kDa subunit	1.43E-02	5.26E-01
ENSBTAG00000037844	CDH18	cadherin 18	1.43E-02	5.26E-01
ENSBTAG00000016740	ACLY	ATP citrate lyase	1.46E-02	5.27E-01
ENSBTAG00000026610	SMCO3	single-pass membrane protein with coiled-coil domains 3	1.46E-02	5.27E-01

ENSBTAG00000002186	NDN	necdin, MAGE family member	1.47E-02	5.27E-01
ENSBTAG00000020315	DENND5B	DENN domain containing 5B	1.48E-02	5.27E-01
ENSBTAG00000006080	MAST1	microtubule associated serine/threonine kinase 1	1.49E-02	5.28E-01
ENSBTAG00000001044	SUPV3L1	Suv3 like RNA helicase	1.52E-02	5.33E-01
ENSBTAG00000021630	MTFMT	mitochondrial methionyl-tRNA formyltransferase	1.52E-02	5.33E-01
ENSBTAG00000004864	CEP89	centrosomal protein 89	1.54E-02	5.34E-01
ENSBTAG00000020150	KLHDC9	kelch domain containing 9	1.56E-02	5.35E-01
ENSBTAG00000004316	BOD1L1	biorientation of chromosomes in cell division 1 like 1	1.56E-02	5.35E-01
ENSBTAG00000011846	TUT1	terminal uridylyl transferase 1, U6 snRNA-specific	1.57E-02	5.35E-01
ENSBTAG00000025136	MYOZ3	myozenin 3	1.64E-02	5.40E-01
ENSBTAG00000003238	MEOX2	mesenchyme homeobox 2	1.64E-02	5.40E-01
ENSBTAG00000004856	RNF130	ring finger protein 130	1.64E-02	5.40E-01
ENSBTAG00000014804	HNRNPDL	heterogeneous nuclear ribonucleoprotein D like	1.65E-02	5.40E-01
ENSBTAG00000046430	ZNF804B	zinc finger protein 804B	1.69E-02	5.44E-01
ENSBTAG00000006008	CAMSAP1	calmodulin regulated spectrin associated protein 1	1.71E-02	5.45E-01
ENSBTAG00000013284	SGK3	serum/glucocorticoid regulated kinase family, member 3	1.71E-02	5.46E-01
ENSBTAG00000012250	BLOC1S6	biogenesis of lysosomal organelles complex 1 subunit 6	1.72E-02	5.46E-01
ENSBTAG00000012938	JARID2#	jumonji and AT-rich interaction domain containing 2	1.73E-02	5.46E-01
ENSBTAG00000004715	AKIRIN1	akirin 1	1.74E-02	5.46E-01
ENSBTAG00000036127	AS3MT	arsenite methyltransferase	1.75E-02	5.46E-01
ENSBTAG00000014861	SLC20A2	solute carrier family 20 member 2	1.77E-02	5.46E-01
ENSBTAG00000017128	NUP153	nucleoporin 153	1.78E-02	5.46E-01
ENSBTAG00000011324	EMILIN1	elastin microfibril interfacer 1	1.78E-02	5.46E-01
ENSBTAG00000018549	SPAG16	NA	1.82E-02	5.46E-01
ENSBTAG00000011843	EEF1G	eukaryotic translation elongation factor 1 gamma	1.82E-02	5.46E-01
ENSBTAG00000021180	TBATA	thymus, brain and testes associated	1.83E-02	5.46E-01
ENSBTAG00000020120	SEL1L2	SEL1L2 ERAD E3 ligase adaptor subunit	1.84E-02	5.46E-01
ENSBTAG00000047443	BRDT	NA	1.85E-02	5.46E-01
ENSBTAG00000020264	CCDC181	coiled-coil domain containing 181	1.86E-02	5.46E-01
ENSBTAG00000047119	SLC29A3	equilibrative nucleoside transporter 3-like	1.87E-02	5.46E-01
ENSBTAG00000007834	PPP1R16A	protein phosphatase 1 regulatory subunit 16A	1.95E-02	5.57E-01
ENSBTAG00000006662	ADAMTSL5	NA	1.97E-02	5.59E-01
ENSBTAG00000030518	ECSCR	endothelial cell surface expressed chemotaxis and apoptosis regulator	1.97E-02	5.59E-01

ENSBTAG00000012615	ZEB2	NA	1.99E-02	5.59E-01
ENSBTAG00000048087	LOC101902869	signal-regulatory protein beta-1 isoform 3-like	2.01E-02	5.62E-01
ENSBTAG00000009279	TNKS2	tankyrase 2	2.02E-02	5.62E-01
ENSBTAG00000018134	AREG	amphiregulin	2.04E-02	5.63E-01
ENSBTAG00000011101	EML6	echinoderm microtubule associated protein like 6	2.05E-02	5.63E-01
ENSBTAG00000011096	ERGIC2	ERGIC and golgi 2	2.07E-02	5.66E-01
ENSBTAG00000006612	SCAF1	SR-related CTD associated factor 1	2.07E-02	5.66E-01
ENSBTAG00000046051	IGSF10	immunoglobulin superfamily member 10-like	2.09E-02	5.70E-01
ENSBTAG00000035662	CAMK4	calcium/calmodulin dependent protein kinase IV	2.10E-02	5.71E-01
ENSBTAG00000018973	COPS3	COP9 signalosome subunit 3	2.12E-02	5.73E-01
ENSBTAG00000010676	RBM44	RNA binding motif protein 44	2.14E-02	5.75E-01
ENSBTAG00000010351	SNX25	sorting nexin 25	2.16E-02	5.77E-01
ENSBTAG00000025191	SKP1	S-phase kinase associated protein 1	2.19E-02	5.78E-01
ENSBTAG00000019492	FANCE	Fanconi anemia complementation group E	2.22E-02	5.83E-01
ENSBTAG00000038523	ATP1A4	ATPase Na+/K+ transporting subunit alpha 4	2.24E-02	5.83E-01
ENSBTAG00000000958	ZSWIM3	zinc finger SWIM-type containing 3	2.27E-02	5.83E-01
ENSBTAG00000007933	C1H3orf58	chromosome 1 open reading frame, human C3orf58	2.28E-02	5.83E-01
ENSBTAG00000008390	DNAJC10	DnaJ heat shock protein family (Hsp40) member C10	2.29E-02	5.83E-01
ENSBTAG00000019065	EEPD1	endonuclease/exonuclease/phosphatase family domain containing 1	2.30E-02	5.83E-01
ENSBTAG00000004873	CCNL2	cyclin L2	2.31E-02	5.83E-01
ENSBTAG00000025021	FMN2	formin 2	2.31E-02	5.83E-01
ENSBTAG00000014391	CRB2	crumbs 2, cell polarity complex component	2.31E-02	5.83E-01
ENSBTAG00000006158	DZIP3	DAZ interacting zinc finger protein 3	2.32E-02	5.83E-01
ENSBTAG00000038333	RBM23	RNA binding motif protein 23	2.38E-02	5.89E-01
ENSBTAG00000033186	OXCT1	3-oxoacid CoA-transferase 1	2.40E-02	5.89E-01
ENSBTAG00000038597	LOC528373	putative olfactory receptor 2W6	2.41E-02	5.89E-01
ENSBTAG00000013472	COL1A2	collagen type I alpha 2 chain	2.43E-02	5.89E-01
ENSBTAG00000013060	IQGAP1	IQ motif containing GTPase activating protein 1	2.43E-02	5.89E-01
ENSBTAG00000010533	HMGXB4	HMG-box containing 4	2.44E-02	5.89E-01
ENSBTAG00000021961	SPR	sepiapterin reductase (7,8-dihydrobiopterin:NADP+ oxidoreductase)	2.45E-02	5.91E-01
ENSBTAG00000001947	ZNF514	zinc finger protein 514	2.46E-02	5.92E-01
ENSBTAG00000010227	CPSF2	cleavage and polyadenylation specific factor 2	2.51E-02	5.94E-01

ENSBTAG00000017799	PITPNB	phosphatidylinositol transfer protein beta	2.56E-02	5.99E-01
ENSBTAG00000017326	OMA1	OMA1 zinc metallopeptidase	2.58E-02	6.02E-01
ENSBTAG00000005838	ULK3	unc-51 like kinase 3	2.58E-02	6.02E-01
ENSBTAG00000005483	ESYT2	extended synaptotagmin 2	2.63E-02	6.02E-01
ENSBTAG00000008359	FKBP2	NA	2.63E-02	6.02E-01
ENSBTAG00000005166	CHTOP	chromatin target of PRMT1	2.64E-02	6.02E-01
ENSBTAG00000014102	WDR77	WD repeat domain 77	2.65E-02	6.02E-01
ENSBTAG00000021817	C13H20orf141	chromosome 13 C20orf141 homolog	2.65E-02	6.02E-01
ENSBTAG00000012476	NRBF2	nuclear receptor binding factor 2	2.65E-02	6.02E-01
ENSBTAG00000003506	STEAP2	STEAP2 metalloreductase	2.67E-02	6.02E-01
ENSBTAG00000019700	PC	pyruvate carboxylase	2.68E-02	6.02E-01
ENSBTAG00000020407	MTSS1	MTSS1, I-BAR domain containing	2.70E-02	6.02E-01
ENSBTAG00000017715	HOMER2	homer scaffolding protein 2	2.72E-02	6.02E-01
ENSBTAG00000013393	GEMIN4	gem nuclear organelle associated protein 4	2.72E-02	6.02E-01
ENSBTAG00000017762	GNG8	G protein subunit gamma 8	2.74E-02	6.02E-01
ENSBTAG00000022535	GPR139	G protein-coupled receptor 139	2.75E-02	6.02E-01
ENSBTAG00000034225	TAF5L	TAF5-like RNA polymerase II p300/CBP-associated factor-associated factor 65 kDa subunit 5L pseudogene	2.77E-02	6.02E-01
ENSBTAG00000012780	LPO#	lactoperoxidase	2.78E-02	6.02E-01
ENSBTAG00000012197	AP5Z1	adaptor related protein complex 5 zeta 1 subunit	2.78E-02	6.02E-01
ENSBTAG00000008333	ETV4	ETS variant 4	2.78E-02	6.02E-01
ENSBTAG00000007284	CCNA1	cyclin A1	2.78E-02	6.02E-01
ENSBTAG00000006188	USH2A	usherin	2.82E-02	6.07E-01
ENSBTAG00000021064	AKAP13	NA	2.84E-02	6.07E-01
ENSBTAG00000015885	PPFIA4	PTPRF interacting protein alpha 4	2.84E-02	6.07E-01
ENSBTAG00000015669	ADAT1	adenosine deaminase, tRNA specific 1	2.84E-02	6.07E-01
ENSBTAG00000001810	SCAF11	SR-related CTD associated factor 11	2.87E-02	6.07E-01
ENSBTAG00000026032	ZYG11A	zyg-11 family member A, cell cycle regulator	2.88E-02	6.07E-01
ENSBTAG00000005940	PRKAB1	protein kinase AMP-activated non-catalytic subunit beta 1	2.88E-02	6.07E-01
ENSBTAG00000017713	KTN1	kinectin 1	2.89E-02	6.07E-01
ENSBTAG00000032289	ARHGAP15#	Rho GTPase activating protein 15	2.90E-02	6.07E-01
ENSBTAG00000000737	DMXL2	NA	2.91E-02	6.07E-01
ENSBTAG00000039461	MS4A15	NA	2.94E-02	6.07E-01
ENSBTAG00000016594	PIGQ	phosphatidylinositol glycan anchor biosynthesis class Q	2.97E-02	6.07E-01

ENSBTAG00000023289	SLC26A10	NA	2.98E-02	6.07E-01
ENSBTAG00000017482	ISYNA1	inositol-3-phosphate synthase 1	2.98E-02	6.07E-01
ENSBTAG00000003096	OR6K3	olfactory receptor, family 6, subfamily K, member 3	3.03E-02	6.07E-01
ENSBTAG00000008749	OLIG3	oligodendrocyte transcription factor 3	3.05E-02	6.07E-01
ENSBTAG00000022731	SSR1	signal sequence receptor subunit 1	3.06E-02	6.07E-01
ENSBTAG00000020385	ALDH1B1	aldehyde dehydrogenase 1 family member B1	3.13E-02	6.07E-01
ENSBTAG00000019152	NYAP2	NA	3.14E-02	6.07E-01
ENSBTAG00000001096	PRKRA	protein activator of interferon induced protein kinase EIF2AK2	3.23E-02	6.09E-01
ENSBTAG00000046493	PDCD6	programmed cell death 6	3.23E-02	6.09E-01
ENSBTAG00000016822	PPIB	peptidylprolyl isomerase B	3.24E-02	6.09E-01
ENSBTAG00000038421	NPY5R	neuropeptide Y receptor type 5	3.29E-02	6.12E-01
ENSBTAG00000004840	C1S	complement C1s	3.31E-02	6.12E-01
ENSBTAG00000013483	TAF1A	TATA-box binding protein associated factor, RNA polymerase I subunit A	3.32E-02	6.12E-01
ENSBTAG00000003625	VSTM2A	V-set and transmembrane domain containing 2A	3.33E-02	6.12E-01
ENSBTAG00000004327	LONRF2	NA	3.34E-02	6.12E-01
ENSBTAG00000024061	NOTO#	notochord homeobox	3.34E-02	6.12E-01
ENSBTAG00000009641	MTHFD1#	methylenetetrahydrofolate dehydrogenase, cyclohydrolase and formyltetrahydrofolate synthetase 1	3.36E-02	6.12E-01
ENSBTAG00000014807	DPP8	dipeptidyl peptidase 8	3.41E-02	6.13E-01
ENSBTAG00000045787	CDS1	CDP-diacylglycerol synthase 1	3.42E-02	6.13E-01
ENSBTAG00000018940	CRACR2A	calcium release activated channel regulator 2A	3.42E-02	6.13E-01
ENSBTAG00000018256	SMC6	structural maintenance of chromosomes 6	3.44E-02	6.13E-01
ENSBTAG00000032292	CCDC159	coiled-coil domain containing 159	3.45E-02	6.13E-01
ENSBTAG00000018889	ATP6V0B	ATPase H+ transporting V0 subunit b	3.46E-02	6.15E-01
ENSBTAG00000021717	BDKRB2	bradykinin receptor B2	3.46E-02	6.15E-01
ENSBTAG00000001271	PLG	plasminogen	3.51E-02	6.16E-01
ENSBTAG00000006320	DBT	dihydrolipoamide branched chain transacylase E2	3.54E-02	6.19E-01
ENSBTAG00000006346	DAP	death associated protein	3.55E-02	6.19E-01
ENSBTAG00000017026	DEPDC1B	DEP domain containing 1B	3.56E-02	6.19E-01
ENSBTAG00000007228	CBX7	chromobox 7	3.57E-02	6.19E-01
ENSBTAG00000020034	LYN	LYN proto-oncogene, Src family tyrosine kinase	3.63E-02	6.22E-01
ENSBTAG00000015386	REL*	REL proto-oncogene, NF-kB subunit	3.63E-02	6.22E-01
ENSBTAG00000047734	C16orf58	NA	3.66E-02	6.22E-01

ENSBTAG00000004660	SPATS2	spermatogenesis associated serine rich 2	3.68E-02	6.25E-01
ENSBTAG00000027932	BIRC6	baculoviral IAP repeat containing 6	3.75E-02	6.29E-01
ENSBTAG00000001298	STAMBPL1	STAM binding protein like 1	3.75E-02	6.29E-01
ENSBTAG00000047214	TRAPPC1	trafficking protein particle complex 1	3.76E-02	6.29E-01
ENSBTAG00000006581	CCDC82	coiled-coil domain containing 82	3.81E-02	6.33E-01
ENSBTAG00000014377	CHD3	chromodomain helicase DNA binding protein 3	3.82E-02	6.33E-01
ENSBTAG00000034384	VWA3B	von Willebrand factor A domain containing 3B	3.82E-02	6.33E-01
ENSBTAG00000015742	ICAM3	intercellular adhesion molecule 3	3.88E-02	6.35E-01
ENSBTAG00000046169	CPA1	carboxypeptidase A1	3.92E-02	6.35E-01
ENSBTAG00000012099	TMEM87B	transmembrane protein 87B	3.96E-02	6.35E-01
ENSBTAG00000012063	E2F4#	E2F transcription factor 4	3.98E-02	6.35E-01
ENSBTAG00000008338	PLCB1	phospholipase C beta 1	3.99E-02	6.35E-01
ENSBTAG00000001314	TRMT6	tRNA methyltransferase 6	3.99E-02	6.35E-01
ENSBTAG00000019839	LTBP1	latent transforming growth factor beta binding protein 1	4.02E-02	6.35E-01
ENSBTAG00000033555	OR5D18	olfactory receptor 5D18	4.04E-02	6.37E-01
ENSBTAG00000016103	CBFB	core-binding factor beta subunit	4.05E-02	6.37E-01
ENSBTAG00000016060	CREM	cAMP responsive element modulator	4.09E-02	6.37E-01
ENSBTAG00000015252	CHRNA9	cholinergic receptor nicotinic alpha 9 subunit	4.11E-02	6.37E-01
ENSBTAG00000001553	HNRNPA1	heterogeneous nuclear ribonucleoprotein A1-like	4.16E-02	6.40E-01
ENSBTAG00000001578	ADPGK	ADP dependent glucokinase	4.17E-02	6.40E-01
ENSBTAG00000005476	METTL21A	methyltransferase like 21A	4.21E-02	6.40E-01
ENSBTAG00000012271	THAP2	THAP domain containing 2	4.22E-02	6.40E-01
ENSBTAG00000022986	FAM19A5	family with sequence similarity 19 member A5, C-C motif chemokine like	4.23E-02	6.40E-01
ENSBTAG00000011133	AP1S3	adaptor related protein complex 1 sigma 3 subunit	4.26E-02	6.40E-01
ENSBTAG00000001825	SP6	Sp6 transcription factor	4.26E-02	6.40E-01
ENSBTAG00000047009	ANKRD66	ankyrin repeat domain 66	4.28E-02	6.41E-01
ENSBTAG00000006998	RASGRP4	RAS guanyl releasing protein 4	4.29E-02	6.41E-01
ENSBTAG00000010234	DHRS1	dehydrogenase/reductase 1	4.31E-02	6.41E-01
ENSBTAG00000003257	STK4	serine/threonine kinase 4	4.33E-02	6.41E-01
ENSBTAG00000008952	RAP1GAP	RAP1 GTPase activating protein	4.33E-02	6.41E-01
ENSBTAG00000044132	NTN5	netrin 5	4.34E-02	6.41E-01
ENSBTAG00000037461	SDHAF1	succinate dehydrogenase complex assembly factor 1	4.34E-02	6.41E-01
ENSBTAG00000010627	SF3B3	splicing factor 3b subunit 3	4.35E-02	6.41E-01

ENSBTAG00000019130	FAM149B1	family with sequence similarity 149 member B1	4.35E-02	6.41E-01
ENSBTAG00000021051	ZNHIT6	zinc finger HIT-type containing 6	4.35E-02	6.41E-01
ENSBTAG00000012039	PHACTR1	phosphatase and actin regulator 1	4.37E-02	6.41E-01
ENSBTAG00000014809	ANXA6	annexin A6	4.40E-02	6.42E-01
ENSBTAG00000013982	UACA	uveal autoantigen with coiled-coil domains and ankyrin repeats	4.41E-02	6.42E-01
ENSBTAG00000006740	SCYL1	SCY1 like pseudokinase 1	4.44E-02	6.42E-01
ENSBTAG00000008409	MYC#	v-myc avian myelocytomatosis viral oncogene homolog	4.45E-02	6.42E-01
ENSBTAG00000038476	HIST2H2AB	histone cluster 2, H2ab	4.45E-02	6.42E-01
ENSBTAG00000040497	LIN28A	lin-28 homolog A	4.48E-02	6.42E-01
ENSBTAG00000004409	IVD	isovaleryl-CoA dehydrogenase	4.51E-02	6.44E-01
ENSBTAG00000048315	OR2C3	olfactory receptor 2C3	4.51E-02	6.44E-01
ENSBTAG00000018399	MYH15	myosin heavy chain 15	4.53E-02	6.44E-01
ENSBTAG00000008541	MGST1	microsomal glutathione S-transferase 1	4.53E-02	6.44E-01
ENSBTAG00000001343	DEPDC1	DEP domain-containing protein 1A	4.55E-02	6.44E-01
ENSBTAG00000011176	TPRKB	TP53RK binding protein	4.56E-02	6.44E-01
ENSBTAG00000036222	NINL	ninein like	4.59E-02	6.44E-01
ENSBTAG00000017361	BAG5	BCL2 associated athanogene 5	4.60E-02	6.44E-01
ENSBTAG00000022751	ZCWPW2	zinc finger CW-type and PWWP domain containing 2	4.61E-02	6.44E-01
ENSBTAG00000020533	FBXO34	F-box protein 34	4.62E-02	6.44E-01
ENSBTAG00000010984	CDKN2AIPNL	CDKN2A interacting protein N-terminal like	4.63E-02	6.44E-01
ENSBTAG00000033345	STAR	steroidogenic acute regulatory protein	4.66E-02	6.44E-01
ENSBTAG00000005909	LEPROT	leptin receptor overlapping transcript	4.70E-02	6.44E-01
ENSBTAG00000017894	CAD	carbamoyl-phosphate synthetase 2, aspartate transcarbamylase, and dihydroorotase	4.70E-02	6.44E-01
ENSBTAG00000033961	RNF217	NA	4.80E-02	6.49E-01
ENSBTAG00000002233	CPNE2	copine 2	4.81E-02	6.49E-01
ENSBTAG00000012143	TECPR2	tectonin beta-propeller repeat containing 2	4.81E-02	6.49E-01
ENSBTAG00000017992	CD164	CD164 molecule	4.81E-02	6.49E-01
ENSBTAG00000013369	COL14A1	collagen type XIV alpha 1 chain	4.82E-02	6.49E-01
ENSBTAG00000021653	TRIP12	thyroid hormone receptor interactor 12	4.83E-02	6.49E-01
ENSBTAG00000014587	CAGE1	cancer antigen 1	4.83E-02	6.49E-01
ENSBTAG00000021931	C19H17orf49	chromosome 19 open reading frame, human C17orf49	4.89E-02	6.49E-01
ENSBTAG00000035710	ZBBX	NA	4.90E-02	6.49E-01
ENSBTAG00000019454	ANGEL1	angel homolog 1	4.93E-02	6.50E-01

ENSBTAG00000039190	SLC9A5	solute carrier family 9 member A5	4.95E-02	6.50E-01
ENSBTAG00000003895	CYBA	cytochrome b-245, alpha polypeptide	4.96E-02	6.50E-01

Table S15| Enrichment analysis of positively selected genes and rapidly evolving genes in giraffe. Items with *p*-value < 0.05 based on the accumulative hypergeometric distribution are listed.

Category	ID	Description	Input	InGO	*p*-value
KEGG Pathway	hsa04350	TGF-beta signaling pathway	6	67	4.86E-03
KEGG Pathway	hsa04713	Circadian entrainment	6	68	8.80E-03
GO Biological Processes	GO:1903055	positive regulation of extracellular matrix organization	5	21	3.38E-05
GO Biological Processes	GO:1901724	positive regulation of cell proliferation involved in kidney development	3	8	3.29E-04
GO Biological Processes	GO:0048545	response to steroid hormone	17	386	9.41E-04
GO Biological Processes	GO:0014841	skeletal muscle satellite cell proliferation	3	14	1.97E-03
GO Biological Processes	GO:0071560	cellular response to transforming growth factor beta stimulus	12	247	2.31E-03
GO Biological Processes	GO:0030431	sleep	4	34	3.46E-03
GO Biological Processes	GO:0001841	neural tube formation	7	106	3.59E-03
GO Biological Processes	GO:0072073	kidney epithelium development	8	142	5.03E-03
GO Biological Processes	GO:0045777	positive regulation of blood pressure	4	38	5.19E-03
GO Biological Processes	GO:0060393	regulation of pathway-restricted SMAD protein phosphorylation	5	62	5.78E-03
GO Biological Processes	GO:0050772	positive regulation of axonogenesis	6	88	5.87E-03
GO Biological Processes	GO:0035089	establishment of apical/basal cell polarity	3	21	6.53E-03
GO Biological Processes	GO:0051321	meiotic cell cycle	11	251	7.39E-03
GO Biological Processes	GO:0060538	skeletal muscle organ development	8	167	1.28E-02
GO Biological Processes	GO:0007423	sensory organ development	18	554	1.57E-02
GO Biological Processes	GO:0070306	lens fiber cell differentiation	3	29	1.61E-02
GO Biological Processes	GO:0046488	phosphatidylinositol metabolic process	8	177	1.76E-02
GO Biological Processes	GO:0043583	ear development	9	224	2.42E-02
GO Biological Processes	GO:0021955	central nervous system neuron axonogenesis	3	35	2.66E-02
GO Biological Processes	GO:0045494	photoreceptor cell maintenance	3	39	3.52E-02
GO Biological Processes	GO:0030239	myofibril assembly	4	68	3.73E-02

GO Biological Processes	GO:0090184	positive regulation of kidney development	3	40	3.75E-02
GO Biological Processes	GO:0001990	regulation of systemic arterial blood pressure by hormone	3	40	3.75E-02
GO Biological Processes	GO:0048568	embryonic organ development	14	445	3.87E-02
GO Biological Processes	GO:0019226	transmission of nerve impulse	4	70	4.08E-02
GO Cellular Components	GO:0044420	extracellular matrix component	6	54	4.73E-04
GO Cellular Components	GO:0062023	collagen-containing extracellular matrix	17	410	1.79E-03
GO Cellular Components	GO:0019897	extrinsic component of plasma membrane	9	161	3.16E-03
GO Cellular Components	GO:0016607	nuclear speck	16	400	3.43E-03
GO Cellular Components	GO:0035770	ribonucleoprotein granule	11	231	4.02E-03
GO Cellular Components	GO:0031012	extracellular matrix	19	535	5.48E-03
GO Cellular Components	GO:0000151	ubiquitin ligase complex	12	286	7.36E-03
GO Cellular Components	GO:0097730	non-motile cilium	8	155	8.39E-03
GO Cellular Components	GO:0036464	cytoplasmic ribonucleoprotein granule	10	221	8.41E-03
GO Molecular Functions	GO:0008017	microtubule binding	12	255	2.99E-03
GO Molecular Functions	GO:0004386	helicase activity	9	161	3.16E-03
GO Molecular Functions	GO:0004935	adrenergic receptor activity	3	19	4.89E-03
GO Molecular Functions	GO:0015631	tubulin binding	14	347	5.57E-03
GO Molecular Functions	GO:0003779	actin binding	16	431	6.93E-03

Table S16| Rapidly evolving KEGG pathways in giraffe. Items with one-sided binomial test *p*-value < 0.05 are listed.

		Giraffe			Okapi			
KEGG ID	**Pathway name**	**Ka/Ks**	**Count of non-synonymous mutations**	**Count of synonymous mutations**	**Ka/Ks**	**Count of non-synonymous mutations**	**Count of synonymous mutations**	***p*-value**
KO03440	Homologous recombination	0.3550	212.4077	204.8451	0.2001	119.7886	204.9760	5.07E-08
KO04640	Hematopoietic cell lineage	0.1933	115.3414	205.4346	0.1093	72.2523	227.6775	8.24E-06
KO04120	Ubiquitin mediated proteolysis	0.0869	141.1208	574.9287	0.0545	102.8639	668.5956	9.44E-06
KO04611	Platelet activation	0.0745	228.5750	946.0458	0.0529	174.7762	1019.4728	3.87E-05
KO04672	Intestinal immune network for IgA production	0.1686	37.6197	72.6479	0.0706	19.0205	87.7510	4.46E-05
KO04916	Melanogenesis	0.0518	93.8550	527.4902	0.0331	58.8743	518.4286	2.92E-04
KO05020	Prion diseases	0.1384	76.4692	164.4975	0.0809	47.5508	174.9695	4.40E-04
KO05323	Rheumatoid arthritis	0.1079	65.4284	208.3265	0.0635	48.1639	260.5973	7.81E-04
KO05150	Staphylococcus aureus infection	0.1981	71.3655	111.3588	0.1168	62.9234	166.4817	1.37E-03
KO04610	Complement and coagulation cascades	0.2612	222.0129	267.2578	0.1943	225.6995	365.1684	3.07E-03
KO00512	Mucin type O-glycan biosynthesis	0.1110	36.6999	108.5663	0.0620	28.8192	152.6217	3.58E-03
KO05140	Leishmaniasis	0.1301	69.5575	174.2262	0.0886	63.4450	233.4643	9.44E-03
KO04964	Proximal tubule bicarbonate reclamation	0.0669	24.8972	117.5277	0.0380	18.8614	156.6845	1.43E-02
KO04961	Endocrine and other factor-regulated calcium reabsorption	0.0469	42.1161	267.7459	0.0308	32.0577	310.1165	1.84E-02
KO00020	Citrate cycle (TCA cycle)	0.0761	39.8000	172.4155	0.0516	33.2013	211.9826	3.09E-02
KO05133	Pertussis	0.1091	69.3256	198.7527	0.0802	72.9693	284.7039	3.91E-02
KO04261	Adrenergic signaling in cardiomyocytes	0.0433	104.2171	716.1187	0.0342	81.7561	711.7708	4.01E-02

Table S17| Genes containing most unique substitutions (more than 3 sites) at functional domains in giraffe among all ruminants. The "Gene ID" column represents the gene ids in cattle (*Bos taurus*).

Gene ID	Gene symbol	Number of unique substitutions
ENSBTAG00000027464	*FGFRL1**	7
ENSBTAG00000031209	*SLC22A4*	6
ENSBTAG00000009641	*MTHFD1**	6
ENSBTAG00000015170	*LCT*	6
ENSBTAG00000015405	*DCHS1*	6
ENSBTAG00000010229	*LAMA2*	6
ENSBTAG00000017452	*RCAN3**	5
ENSBTAG00000001444	*TNXB*	5
ENSBTAG00000037566	*ZNF500*	5
ENSBTAG00000020725	*CNGA2*	4
ENSBTAG00000025424	*NOTCH4**	4
ENSBTAG00000011032	*MCPH1*	4
ENSBTAG00000006050	*BOLA1*	3
ENSBTAG00000011613	*PLS3*	3
ENSBTAG00000032289	*ARHGAP15**	3
ENSBTAG00000003275	*ANK1*	3
ENSBTAG00000006507	*ADAMTS3*	3
ENSBTAG00000008373	*ITGA10**	3
ENSBTAG00000014903	*ABCA3*	3
ENSBTAG00000016525	*ITGA1*	3
ENSBTAG00000012808	*MASP2*	3
ENSBTAG00000018912	*ARHGEF1*	3
ENSBTAG00000007237	*BUB1B*	3
ENSBTAG00000014112	*EXOC4*	3
ENSBTAG00000019492	*FANCE*	3
ENSBTAG00000000988	*BRCA2*	3
ENSBTAG00000019807	*COL27A1*	3
ENSBTAG00000018010	*ABCA4*	3
ENSBTAG00000012925	*NCAPH*	3
ENSBTAG00000017122	*HSPG2*	3
ENSBTAG00000021125	*NUP160*	3
ENSBTAG00000039346	*ALPP*	3
ENSBTAG00000010077	*FANCD2*	3

* represents genes among the 70 highly divergent genes in giraffe reported by the previous study (*7*).

Table S18| 63 uniquely lost genes in giraffe compared to okapi.

Chromosome in cattle	Gene ID of cattle	CDS length (bp)	Lost length in giraffe (bp)	Lost length in okapi (bp)	Gene symbol
1	ENSBTAG00000022908	978	943	0	*OR5H2*
1	ENSBTAG00000016306	399	217	0	*PFDN4*
4	ENSBTAG00000033359	405	263	0	*HIST1H2BC*
5	ENSBTAG00000021122	936	863	0	*OR6C2*
6	ENSBTAG00000038214	927	705	0	*SULT1D1*
7	ENSBTAG00000040610	939	508	0	*OR5W2*
7	ENSBTAG00000046397	993	788	0	*OR7A5*
7	ENSBTAG00000045623	1,035	1,035	0	*OR2T27*
10	ENSBTAG00000009039	972	969	0	*OR4K5*
10	ENSBTAG00000039370	921	900	0	*OR4K1*
10	ENSBTAG00000046009	954	954	0	*OR4F21*
10	ENSBTAG00000046370	915	915	0	*OR4K15*
10	ENSBTAG00000047566	939	939	0	*OR4K15*
10	ENSBTAG00000038188	939	916	0	*OR4F6*
10	ENSBTAG00000013255	981	981	0	*OR4F17*
10	ENSBTAG00000046207	936	845	0	*OR4F21*
10	ENSBTAG00000047465	933	557	0	*OR4F21*
11	ENSBTAG00000045514	441	352	0	*IGKV1D-13*
14	ENSBTAG00000048001	957	649	0	*OR5D13*
15	ENSBTAG00000046894	612	612	0	*OR10A6*
15	ENSBTAG00000048176	933	929	0	*OR*
15	ENSBTAG00000037603	951	480	0	*OR6*
15	ENSBTAG00000038031	936	896	0	*OR*
15	ENSBTAG00000023912	972	972	0	*OR52N4*
15	ENSBTAG00000038637	942	942	0	*OR51I2*
15	ENSBTAG00000039088	951	951	0	*OR51I2*
15	ENSBTAG00000037992	966	752	0	*OR51Q1*
15	ENSBTAG00000019544	942	923	0	*OR51I1*
15	ENSBTAG00000012546	942	915	0	*OR4C13*
15	ENSBTAG00000031119	927	907	0	*OR4S1*
15	ENSBTAG00000012549	936	525	0	*OR4C3*
15	ENSBTAG00000031032	930	875	0	*OR4C12*
15	ENSBTAG00000030909	849	811	0	*OR4C12*
15	ENSBTAG00000039821	984	588	0	*OR4C13*
15	ENSBTAG00000046923	939	760	0	*OR140*
15	ENSBTAG00000040425	930	745	0	*OR5W2*
15	ENSBTAG00000040341	930	930	0	*OR5W2*
15	ENSBTAG00000005624	909	909	0	*OR5W2*
15	ENSBTAG00000007944	945	907	0	*OR5I1*

15	ENSBTAG00000014594	978	861	0	*OR10AG1*
15	ENSBTAG00000046471	945	837	0	*OR5F1*
15	ENSBTAG00000023511	957	872	0	*OR5F1*
15	ENSBTAG00000048141	963	959	0	*OR10AG1*
15	ENSBTAG00000005874	957	957	0	*OR5F1*
15	ENSBTAG00000035988	942	663	0	*OR8K3*
15	ENSBTAG00000045723	942	893	0	*OR8K3*
15	ENSBTAG00000046167	945	916	0	*OR5J2*
15	ENSBTAG00000024952	945	943	0	*OR5AK2*
17	ENSBTAG00000046986	1,215	985	0	*PRAME*
18	ENSBTAG00000030440	357	328	0	*ZNF738*
18	ENSBTAG00000037710	1,353	1,054	0	*ZNF267*
20	ENSBTAG00000047333	990	843	0	*OR5D13*
20	ENSBTAG00000004920	210	113	0	*COX8A*
22	ENSBTAG00000045666	942	667	0	*OR5D13*
22	ENSBTAG00000023918	909	908	0	*Vomeronasal type-1 receptor*
22	ENSBTAG00000017173	975	975	0	*vomeronasal type-1 receptor 90*
23	ENSBTAG00000000228	948	579	0	*OR2B8*
26	ENSBTAG00000023549	1,473	1,093	0	*CYP2C19*
26	ENSBTAG00000005267	942	787	0	*OR13A1*
28	ENSBTAG00000011707	981	961	0	*OR5AS1*
29	ENSBTAG00000039676	969	528	0	*OR8A1*
X	ENSBTAG00000047194	372	372	0	*TRMT112*
X	ENSBTAG00000025952	525	512	0	*OBP*

Table S19| KEGG pathway and GO enrichment of expanded gene families in giraffe. Items with Fisher's exact test FDR (Banjamini-Hochberg method) value < 0.05 are listed.

Database	Terms	Function	FDR value
KEGG Pathway	bta05322	Systemic lupus erythematosus	3.98E-13
KEGG Pathway	bta00982	Drug metabolism - cytochrome P450	5.44E-06
KEGG Pathway	bta04970	Salivary secretion	5.77E-05
KEGG Pathway	bta04971	Gastric acid secretion	3.61E-03
Gene Ontology	GO:0042742	Defense response to bacterium	4.40E-10

Table S20| KEGG pathway and GO enrichment of contracted gene families in giraffe. Items with Fisher's exact test FDR (Banjamini-Hochberg method) value < 0.05 are listed**.**

Database	Terms	Function	FDR value
KEGG Pathway	bta04740	Olfactory transduction	2.26E-208
KEGG Pathway	bta00730	Thiamine metabolism	0.020897
KEGG Pathway	bta04540	Gap junction	0.039595
Gene Ontology	GO:0004984	olfactory receptor activity	5.79E-76
Gene Ontology	GO:0004930	G protein-coupled receptor activity	6.06E-61
Gene Ontology	GO:0042221	response to chemical	4.67E-18
Gene Ontology	GO:0005200	structural constituent of cytoskeleton	0.000816
Gene Ontology	GO:0051716	cellular response to stimulus	0.001911
Gene Ontology	GO:0005549	odorant binding	0.002393

Table S21| The oligonucleotides used for sgRNA expression vectors.

Item	Name	Sequence
Targeting site 1	M- FGFRL1-EA-gRNA up	5’-TAGGCTCAAGTGTGTGGCCAGT-3’
	M- FGFRL1-EA-gRNA dw	5’-AAACACTGGCCACACACTTGAG-3’
Targeting site 2	M- FGFRL1-EB-gRNA up	5’-TAGGTGGAGTTGTGGCGTCCCT-3’
	M- FGFRL1-EB-gRNA dw	5’-AAACAGGGACGCCACAACTCCA-3’

Table S22| Primers used for amplifying and sequencing CRISPR/Cas9-induced mutations in mice.

Location	Name	Sequence (5'-3')	Amplicon
Upstream	M- Rrm1-EA-F1	GAGTTCAGTTCCCAGCAACC	1,346 bp
	M- Rrm1-EA-R1	CCTCCTACTCACACCAACAGG	
Downstream	M-FGFRL1-DwF1	GGTGGACTTCGGTGGGACAA	959 bp
	M-FGFRL1-DwR1	ATGCTGGTGTTGATGAACCTTGC	

REFERENCES AND NOTES

1. E. Z. Cameron, J. T. du Toit, Winning by a neck: Tall giraffes avoid competing with shorter browsers. *Am. Nat.* **169**, 130–135 (2007).

2. J. P. Coimbra, N. S. Hart, S. P. Collin, P. R. Manger, Scene from above: Retinal ganglion cell topography and spatial resolving power in the giraffe (Giraffa camelopardalis). *J. Comp. Neurol.* **521**, 2042–2057 (2013).

3. G. Mitchell, J. D. Skinner, An allometric analysis of the giraffe cardiovascular system. *Comp. Biochem. Physiol. A Mol. Integr. Physiol.* **154**, 523–529 (2009).

4. E. Brondum, J. M. Hasenkam, N. H. Secher, M. F. Bertelsen, C. Grondahl, K. K. Petersen, R. Buhl, C. Aalkjaer, U. Baandrup, H. Nygaard, M. Smerup, F. Stegmann, E. Sloth, K. H. Ostergaard, P. Nissen, M. Runge, K. Pitsillides, T. Wang, Jugular venous pooling during lowering of the head affects blood pressure of the anesthetized giraffe. *Am. J. Physiol. Regul. Integr. Comp. Physiol.* **297**, R1058–R1065 (2009).

5. H. L. More, S. M. O'Connor, E. Brondum, T. Wang, M. F. Bertelsen, C. Grondahl, K. Kastberg, A. Horlyck, J. Funder, J. M. Donelan, Sensorimotor responsiveness and resolution in the giraffe. *J. Exp. Biol.* **216**, 1003–1011 (2013).

6. H. Endo, D. Yamagiwa, M. Fujisawa, J. Kimura, M. Kurohmaru, Y. Hayashi, Modified neck muscular system of the giraffe (Giraffa camelopardalis). *Ann. Anat.* **179**, 481–485 (1997).

7. M. Agaba, E. Ishengoma, W. C. Miller, B. C. McGrath, C. N. Hudson, O. C. Bedoya Reina, A. Ratan, R. Burhans, R. Chikhi, P. Medvedev, C. A. Praul, L. Wu-Cavener, B. Wood, H. Robertson, L. Penfold, D. R. Cavener, Giraffe genome sequence reveals clues to its unique morphology and physiology. *Nat. Commun.* **7**, 11519 (2016).

8. S. Mallick, S. Gnerre, P. Muller, D. Reich, The difficulty of avoiding false positives in genome scans for natural selection. *Genome Res.* **19**, 922–933 (2009).

9. L. Chen, Q. Qiu, Y. Jiang, K. Wang, Z. Lin, Z. Li, F. Bibi, Y. Yang, J. Wang, W. Nie, W. Su, G. Liu, Q. Li, W. Fu, X. Pan, C. Liu, J. Yang, C. Zhang, Y. Yin, Y. Wang, Y. Zhao, C. Zhang, Z. Wang, Y. Qin, W. Liu, B. Wang, Y. Ren, R. Zhang, Y. Zeng, R. R. da Fonseca, B. Wei, R. Li, W. Wan, R. Zhao, W. Zhu, Y. Wang, S. Duan, Y. Gao, Y. E. Zhang, C. Chen, C. Hvilsom, C. W. Epps, L. G. Chemnick, Y. Dong, S. Mirarab, H. R. Siegismund, O. A. Ryder, M. T. P. Gilbert, H. A. Lewin, G. Zhang, R. Heller, W. Wang, Large-scale ruminant genome sequencing provides insights into their evolution and distinct traits. *Science* **364**, eaav6202 (2019).

10. E. E. Eichler, D. Sankoff, Structural dynamics of eukaryotic chromosome evolution. *Science* **301**, 793–797 (2003).

11. H. Cernohorska, S. Kubickova, O. Kopecna, A. I. Kulemzina, P. L. Perelman, F. F. B. Elder, T. J. Robinson, A. S. Graphodatsky, J. Rubes, Molecular cytogenetic insights to the phylogenetic affinities of the giraffe (Giraffa camelopardalis) and pronghorn (Antilocapra americana). *Chromosome Res.* **21**, 447–460 (2013).

12. Z. Yang, PAML: A program package for phylogenetic analysis by maximum likelihood. *Comput. Appl. Biosci.* **13**, 555–556 (1997).

13. W. H. Gharib, M. Robinson-Rechavi, The branch-site test of positive selection is surprisingly robust but lacks power under synonymous substitution saturation and variation in GC. *Mol. Biol. Evol.* **30**, 1675–1686 (2013).

14. C. Catela, D. Bilbao-Cortes, E. Slonimsky, P. Kratsios, N. Rosenthal, P. Te Welscher, Multiple congenital malformations of Wolf-Hirschhorn syndrome are recapitulated in Fgfrl1 null mice. *Dis. Model. Mech.* **2**, 283–294 (2009).

15. H. Engbers, J. J. van der Smagt, R. van't Slot, J. R. Vermeesch, R. Hochstenbach, M. Poot, Wolf-Hirschhorn syndrome facial dysmorphic features in a patient with a terminal 4p16.3 deletion telomeric to the WHSCR and WHSCR 2 regions. *Eur. J. Hum. Genet.* **17**, 129–132 (2009).

16. X. Pan, Y. Shao, F. Wu, Y. Wang, R. Xiong, J. Zheng, H. Tian, B. Wang, Y. Wang, Y. Zhang, Z. Han, A. Qu, H. Xu, A. Lu, T. Yang, X. Li, A. Xu, J. Du, Z. Lin, FGF21 prevents angiotensin

II-induced hypertension and vascular dysfunction by activation of ACE2/angiotensin-(1-7) axis in mice. *Cell Metab.* **27**, 1323–1337.e5 (2018).

17. T. Niu, N. Liu, M. Zhao, G. Xie, L. Zhang, J. Li, Y. F. Pei, H. Shen, X. Fu, H. He, S. Lu, X. D. Chen, L. J. Tan, T. L. Yang, Y. Guo, P. J. Leo, E. L. Duncan, J. Shen, Y. F. Guo, G. C. Nicholson, R. L. Prince, J. A. Eisman, G. Jones, P. N. Sambrook, X. Hu, P. M. Das, Q. Tian, X. Z. Zhu, C. J. Papasian, M. A. Brown, A. G. Uitterlinden, Y. P. Wang, S. Xiang, H. W. Deng, Identification of a novel FGFRL1 MicroRNA target site polymorphism for bone mineral density in meta-analyses of genome-wide association studies. *Hum. Mol. Genet.* **24**, 4710–4727 (2015).

18. S. C. F. Rawlinson, D. H. Murray, J. R. Mosley, C. D. P. Wright, J. C. Bredl, L. K. Saxon, N. Loveridge, C. Leterrier, P. Constantin, C. Farquharson, A. A. Pitsillides, Genetic selection for fast growth generates bone architecture characterised by enhanced periosteal expansion and limited consolidation of the cortices but a diminution in the early responses to mechanical loading. *Bone* **45**, 357–366 (2009).

19. O. L. van Schalkwyk, J. D. Skinner, G. Mitchell, A comparison of the bone density and morphology of giraffe (Giraffa camelopardalis) and buffalo (Syncerus caffer) skeletons. *J. Zool.* **264**, 307–315 (1999).

20. M. Damkjaer, T. Wang, E. Brondum, K. H. Ostergaard, U. Baandrup, A. Horlyck, J. M. Hasenkam, M. Smerup, J. Funder, N. Marcussen, C. C. Danielsen, M. F. Bertelsen, C. Grondahl, M. Pedersen, P. Agger, G. Candy, C. Aalkjaer, P. Bie, The giraffe kidney tolerates high arterial blood pressure by high renal interstitial pressure and low glomerular filtration rate. *Acta Physiol. (Oxf.)* **214**, 497–510 (2015).

21. M. J. Maxwell, S. M. Dopheide, S. J. Turner, S. P. Jackson, Shear induces a unique series of morphological changes in translocating platelets: Effects of morphology on translocation dynamics. *Arterioscler. Thromb. Vasc. Biol.* **26**, 663–669 (2006).

22. S. F. Jackson, S. M. Schoenwaelder, Type I phosphoinositide 3-kinases: Potential antithrombotic targets? *Cell. Mol. Life Sci.* **63**, 1085–1090 (2006).

23. Z. Xu, J. Wu, J. Xin, Y. Feng, G. Hu, J. Shen, M. Li, Y. Zhang, H. Xiao, L. Wang, β_3-adrenergic receptor activation induces TGFβ1 expression in cardiomyocytes via the PKG/JNK/c-Jun pathway. *Biochem. Biophys. Res. Commun.* **503**, 146–151 (2018).

24. B. Zhang, M. Li, L. Wang, C. Li, Y. Lou, J. Liu, Y. Liu, Z. Wang, S. Wen, The association between the polymorphisms in a sodium channel gene SCN7A and essential hypertension: A case-control study in the Northern Han Chinese. *Ann. Hum. Genet.* **79**, 28–36 (2015).

25. G. Grassi, S. Padmanabhan, C. Menni, G. Seravalle, W. K. Lee, M. Bombelli, G. Brambilla, F. Quarti-Trevano, C. Giannattasio, G. Cesana, A. Dominiczak, G. Mancia, Association between ADRA1A gene and the metabolic syndrome: Candidate genes and functional counterpart in the PAMELA population. *J. Hypertens.* **29**, 1121–1127 (2011).

26. M. Muszkat, D. Kurnik, J. Solus, G. G. Sofowora, H.-G. Xie, L. Jiang, C. McMunn, P. Ihrie, J. R. Harris, E. P. Dawson, S. M. Williams, A. J. J. Wood, C. M. Stein, Variation in the alpha2B-adrenergic receptor gene (ADRA2B) and its relationship to vascular response in vivo. *Pharmacogenet. Genomics* **15**, 407–414 (2005).

27. M. Hara-Chikuma, A. S. Verkman, Aquaporin-1 facilitates epithelial cell migration in kidney proximal tubule. *J. Am. Soc. Nephrol.* **17**, 39–45 (2006).

28. D. Gordienko, O. Povstyan, K. Sukhanova, M. Raphaël, M. Harhun, Y. Dyskina, V. Lehen'kyi, A. Jama, Z.-L. Lu, R. Skryma, N. Prevarskaya, Impaired P2X signalling pathways in renal microvascular myocytes in genetic hypertension. *Cardiovasc. Res.* **105**, 131–142 (2015).

29. G. Tian, C. Dang, Z. Lu, The change and significance of the Na^+-K^+-ATPase alpha-subunit in ouabain-hypertensive rats. *Hypertens. Res.* **24**, 729–734 (2001).

30. K. C. Ehrlich, M. Lacey, M. Ehrlich, Tissue-specific epigenetics of atherosclerosis-related ANGPT and ANGPTL genes. *Epigenomics* **11**, 169–186 (2019).

31. H. Li, H. Cai, J. Deng, X. Tu, Y. Sun, Z. Huang, Z. Ding, L. Dong, J. Chen, Y. Zang, J. Zhang, TGF-β-mediated upregulation of Sox9 in fibroblast promotes renal fibrosis. *Biochim. Biophys. Acta. Mol. Basis Dis.* **1864**, 520–532 (2018).

32. E. M. Williams, Giraffe stature and neck elongation: Vigilance as an evolutionary mechanism. *Biology (Basel)* **5**, 35 (2016).

33. C. C. Veilleux, E. C. Kirk, Visual acuity in mammals: Effects of eye size and ecology. *Brain Behav. Evol.* **83**, 43–53 (2014).

34. P. Mathur, J. Yang, Usher syndrome: Hearing loss, retinal degeneration and associated abnormalities. *Biochim. Biophys. Acta* **1852**, 406–420 (2015).

35. D. Backhaus, Experimentelle Prüfung des Farbsehvermögens einer Massai-Giraffe (*Giraffa camelopardalis tippelskirchi* Matschie 1898). *Ethology* **16**, 468–477 (1959).

36. S. Nummela, H. Pihlstrom, K. Puolamaki, M. Fortelius, S. Hemila, T. Reuter, Exploring the mammalian sensory space: Co-operations and trade-offs among senses. *J. Comp. Physiol. A Neuroethol. Sens. Neural Behav. Physiol.* **199**, 1077–1092 (2013).

37. J. M. Siegel, Clues to the functions of mammalian sleep. *Nature* **437**, 1264–1271 (2005).

38. A. C. Liu, D. K. Welsh, C. H. Ko, H. G. Tran, E. E. Zhang, A. A. Priest, E. D. Buhr, O. Singer, K. Meeker, I. M. Verma, F. J. Doyle III, J. S. Takahashi, S. A. Kay, Intercellular coupling confers robustness against mutations in the SCN circadian clock network. *Cell* **129**, 605–616 (2007).

39. L. I. Kiyashchenko, B. Y. Mileykovskiy, N. Maidment, H. A. Lam, M. F. Wu, J. John, J. Peever, J. M. Siegel, Release of hypocretin (orexin) during waking and sleep states. *J. Neurosci.* **22**, 5282–5286 (2002).

40. K. Marten, P. Marler, Sound transmission and its significance for animal vocalization: I. Temperate habitats. *Behav. Ecol. Sociobiol.* **2**, 271–290 (1977).

41. J. Ruan, H. Li, Fast and accurate long-read assembly with wtdbg2. *Nat. Methods* **17**, 155–158 (2020).

42. R. Vaser, I. Sovic, N. Nagarajan, M. Sikic, Fast and accurate de novo genome assembly from long uncorrected reads. *Genome Res.* **27**, 737–746 (2017).

43. B. J. Walker, T. Abeel, T. Shea, M. Priest, A. Abouelliel, S. Sakthikumar, C. A. Cuomo, Q. D. Zeng, J. Wortman, S. K. Young, A. M. Earl, Pilon: An integrated tool for comprehensive microbial variant detection and genome assembly improvement. *PLOS ONE* **9**, e112963 (2014).

44. N. C. Durand, M. S. Shamim, I. Machol, S. S. Rao, M. H. Huntley, E. S. Lander, E. L. Aiden, Juicer provides a one-click system for analyzing loop-resolution Hi-C experiments. *Cell Syst.* **3**, 95–98 (2016).

45. O. Dudchenko, S. S. Batra, A. D. Omer, S. K. Nyquist, M. Hoeger, N. C. Durand, M. S. Shamim, I. Machol, E. S. Lander, A. P. Aiden, E. L. Aiden, De novo assembly of the *Aedes aegypti* genome using Hi-C yields chromosome-length scaffolds. *Science* **356**, 92–95 (2017).

46. F. A. Simao, R. M. Waterhouse, P. Ioannidis, E. V. Kriventseva, E. M. Zdobnov, BUSCO: Assessing genome assembly and annotation completeness with single-copy orthologs. *Bioinformatics* **31**, 3210–3212 (2015).

47. L. Huang, A. Nesterenko, W. Nie, J. Wang, W. Su, A. S. Graphodatsky, F. Yang, Karyotype evolution of giraffes (Giraffa camelopardalis) revealed by cross-species chromosome painting with Chinese muntjac (Muntiacus reevesi) and human (Homo sapiens) paints. *Cytogenet. Genome Res.* **122**, 132–138 (2008).

48. Benson, G., Tandem repeats finder: A program to analyze DNA sequences. *Nucleic Acids Res.* **27**, 573–580 (1999).

49. J. A. Bedell, I. Korf, W. Gish, MaskerAid: A performance enhancement to RepeatMasker. *Bioinformatics* **16**, 1040–1041 (2000).

50. M. Stanke, S. Waack, Gene prediction with a hidden Markov model and a new intron submodel. *Bioinformatics* **19**, ii215–ii225 (2003).

51. C. Burge, S. Karlin, Prediction of complete gene structures in human genomic DNA. *J. Mol. Biol.* **268**, 78–94 (1997).

52. S. F. Altschul, W. Gish, W. Miller, E. W. Myers, D. J. Lipman, Basic local alignment search tool. *J. Mol. Biol.* **215**, 403–410 (1990).

53. E. Birney, M. Clamp, R. Durbin, GeneWise and genomewise. *Genome Res.* **14**, 988–995 (2004).

54. B. J. Haas, S. L. Salzberg, W. Zhu, M. Pertea, J. E. Allen, J. Orvis, O. White, C Robin Buell, J. R. Wortman, Automated eukaryotic gene structure annotation using EVidenceModeler and the Program to Assemble Spliced Alignments. *Genome Biol.* **9**, R7 (2008).

55. E. M. Zdobnov, R. Apweiler, InterProScan—An integration platform for the signature-recognition methods in InterPro. *Bioinformatics* **17**, 847–848 (2001).

56. J. Fennessy, T. Bidon, F. Reuss, V. Kumar, P. Elkan, M. A. Nilsson, M. Vamberger, U. Fritz, A. Janke, Multi-locus analyses reveal four giraffe species instead of one. *Curr. Biol.* **26**, 2543–2549 (2016).

57. S. Kumar, G. Stecher, K. Tamura, MEGA7: Molecular evolutionary genetics analysis version 7.0 for bigger datasets. *Mol. Biol. Evol.* **33**, 1870–1874 (2016).

58. B. Q. Minh, H. A. Schmidt, O. Chernomor, D. Schrempf, M. D. Woodhams, A. von Haeseler, R. Lanfear, IQ-TREE 2: New models and efficient methods for phylogenetic inference in the genomic era. *Mol. Biol. Evol.* **37**, 1530–1534 (2020).

59. J. Kim, M. Farre, L. Auvil, B. Capitanu, D. M. Larkin, J. Ma, H. A. Lewin, Reconstruction and evolutionary history of eutherian chromosomes. *Proc. Natl. Acad. Sci. U.S.A.* **114**, E5379–E5388 (2017).

60. S. M. Kielbasa, R. Wan, K. Sato, P. Horton, M. C. Frith, Adaptive seeds tame genomic sequence comparison. *Genome Res.* **21**, 487–493 (2011).

61. M. Blanchette, W. J. Kent, C. Riemer, L. Elnitski, A. F. Smit, K. M. Roskin, R. Baertsch, K. Rosenbloom, H. Clawson, E. D. Green, D. Haussler, W. Miller, Aligning multiple genomic sequences with the threaded blockset aligner. *Genome Res.* **14**, 708–715 (2004).

62. Y. Zhou, B. Zhou, L. Pache, M. Chang, A. H. Khodabakhshi, O. Tanaseichuk, C. Benner, S. K. Chanda, Metascape provides a biologist-oriented resource for the analysis of systems-level datasets. *Nat. Commun.* **10**, 1523 (2019).

63. L. Li, C. J. Stoeckert Jr., D. S. Roos, OrthoMCL: Identification of ortholog groups for eukaryotic genomes. *Genome Res.* **13**, 2178–2189 (2003).

64. T. De Bie, N. Cristianini, J. P. Demuth, M. W. Hahn, CAFE: A computational tool for the study of gene family evolution. *Bioinformatics* **22**, 1269–1271 (2006).

65. C. Xie, X. Mao, J. Huang, Y. Ding, J. Wu, S. Dong, L. Kong, G. Gao, C. Y. Li, L. Wei, KOBAS 2.0: A web server for annotation and identification of enriched pathways and diseases. *Nucleic Acids Res.* **39**, W316–W322 (2011).

66. K. Wang, Y. Shen, Y. Yang, X. Gan, G. Liu, K. Hu, Y. Li, Z. Gao, L. Zhu, G. Yan, L. He, X. Shan, L. Yang, S. Lu, H. Zeng, X. Pan, C. Liu, Y. Yuan, C. Feng, W. Xu, C. Zhu, W. Xiao, Y. Dong, W. Wang, Q. Qiu, S. He, Morphology and genome of a snailfish from the Mariana Trench provide insights into deep-sea adaptation. *Nat. Ecol. Evol.* **3**, 823–833 (2019).

67. S. El-Gebali, J. Mistry, A. Bateman, S. R. Eddy, A. Luciani, S. C. Potter, M. Qureshi, L. J. Richardson, G. A. Salazar, A. Smart, E. L. L. Sonnhammer, L. Hirsh, L. Paladin, D. Piovesan, S. C. E. Tosatto, R. D. Finn, The Pfam protein families database in 2019. *Nucleic Acids Res.* **47**, D427–D432 (2019).

68. H. Li, B. Handsaker, A. Wysoker, T. Fennell, J. Ruan, N. Homer, G. Marth, G. Abecasis, R. Durbin, S. Genome The sequence Alignment/Map format and SAMtools. *Bioinformatics* **25**, 2078–2079 (2009).

69. G. Chen, Y. Liu, R. Goetz, L. Fu, S. Jayaraman, M.-C. Hu, O. W. Moe, G. Liang, X. Li, M. Mohammadi, α-Klotho is a non-enzymatic molecular scaffold for FGF23 hormone signalling. *Nature* **553**, 461–466 (2018).

70. J. Pei, M. Tang, N. V. Grishin, PROMALS3D web server for accurate multiple protein sequence and structure alignments. *Nucleic Acids Res.* **36**, W30–W34 (2008).

71. Y. Song, F. DiMaio, R. Y.-R. Wang, D. Kim, C. Miles, T. Brunette, J. Thompson, D. Baker, High-resolution comparative modeling with RosettaCM. *Structure* **21**, 1735–1742 (2013).

72. D. A. Case, T. E. Cheatham III, T. Darden, H. Gohlke, R. Luo, K. M. Merz, Jr., A. Onufriev, C. Simmerling, B. Wang, R. J. Woods, The Amber biomolecular simulation programs. *J. Comput. Chem.* **26**, 1668–1688 (2005).

73. J. A. Maier, C. Martinez, K. Kasavajhala, L. Wickstrom, K. E. Hauser, C. Simmerling, ff14SB: Improving the accuracy of protein side chain and backbone parameters from ff99SB. *J. Chem. Theory Comput.* **11**, 3696–3713 (2015).

74. M. Farre, Q. Li, I. Darolti, Y. Zhou, J. Damas, A. A. Proskuryakova, A. I. Kulemzina, L. G. Chemnick, J. Kim, O. A. Ryder, J. Ma, A. S. Graphodatsky, G. Zhang, D. M. Larkin, H. A. Lewin, An integrated chromosome-scale genome assembly of the Masai giraffe (Giraffa camelopardalis tippelskirchi). *Gigascience* **8** (2019).

75. I. Letunic, P. Bork, 20 years of the SMART protein domain annotation resource. *Nucleic Acids Res.* **46**, D493–D496 (2018).

76. H. Li, Minimap and miniasm: Fast mapping and de novo assembly for noisy long sequences. *Bioinformatics* **32**, 2103–2110 (2016).